Chemical induction of hypocotyl rooting reveals extensive conservation of auxin signalling controlling lateral and adventitious root formation

Yinwei Zeng[1+], Inge Verstraeten[1+], Hoang Khai Trinh[1,2], Robin Lardon[1], Sebastien Schotte[1], Damilola Olatunji[1], Thomas Heugebaert[3], Christian Stevens[3], Mussa Quareshy[4], Richard Napier[4], Sara Paola Nastasi[5], Alex Costa[5,6], Bert De Rybel[7,8], Catherine Bellini[9,10], Tom Beeckman[7,8], Steffen Vanneste[1], Danny Geelen[1,*]

1. Horticell, Department Plants and Crops, Faculty of Bioscience Engineering, Ghent University, Ghent, Belgium

2. Institute of Food and Biotechnology, Can Tho University, Can Tho City, Vietnam

3. Department of Green Chemistry and Technology, Faculty of Bioscience Engineering, Ghent University, Coupure Links 653, 9000 Ghent, Belgium

4. School of Life Sciences, University of Warwick, Coventry CV4 7AL, UK

5. Department of Biosciences, University of Milan, via Celoria 26, 20133 Milano, Italy

6. Institute of Biophysics, National Research Council of Italy (CNR), 20133 Milano, Italy

7. Ghent University, Department of Plant Biotechnology and Bioinformatics, Technologiepark 71, 9052 Ghent, Belgium

8. VIB Centre for Plant Systems Biology, Technologiepark 71, 9052 Ghent, Belgium

9. Umeå Plant Science Centre, Department of Plant Physiology, Umeå University, SE-90736 Umeå, Sweden;

10. Université Paris-Saclay, INRAE, AgroParisTech, Institut Jean-Pierre Bourgin (IJPB), 78000, Versailles, France

+Equal contribution

*corresponding author: danny.geelen@ugent.be

short title: Conservation of adventitious and lateral root induction

Abstract

Lateral root (LR) branching has been studied intensively, while the ontogeny and initiation of adventitious roots (AR) remains largely unknown. Differences between AR and LR formation were addressed using a small molecule named Hypocotyl Specific Adventitious Root INducer (HYSPARIN; HYS) that shows strong AR inducing capacity in Arabidopsis, tomato, and rice. HYSPARIN does not trigger a rapid molecular response of DR5-reporter activation, DII-Venus degradation or Ca^{2+} signalling. Transcriptome analysis, auxin signalling reporter lines and mutants, show that HYS AR induction involves nuclear TIR1/AFB as well as plasma membrane TMK auxin signalling and multiple downstream LR development genes that include *SHY2/IAA3*, *PUCHI*, *MAKR4* and *GATA23*. Comparison of AR and LR transcriptome data sets identified SAURs, AGC kinases and OFP transcription factors to be specifically upregulated by HYS. Members of the SAUR19 subfamily, OFP4, and AGC2 suppress HYS-induced AR formation. While SAUR19 and OFP subfamily members also mildly modulate LR formation, AGC2 regulates only AR induction. Together, molecular and genetic analysis of HYS-induced AR formation uncovers an evolutionary conservation of auxin signalling that controls LR and AR induction and identifies SAUR19, OFP4 and AGC2 kinase as novel regulators of adventitious root formation.

Introduction

The sessile lifestyle of plants implies a strong dependence on the resources that are in its immediate vicinity. The establishment of a complex root system aims to optimally explore the soil for water and nutrients, to interact with soil microbes, and to provide anchorage.

In plants that establish a taproot system governed by a primary root and lateral roots, a single primary root is specified during embryogenesis. During the growth of the primary root, external and internal cues specify the position where new lateral roots develop, which in turn grow and branch to iteratively establish a complex root system (Lynch 1995, Zhang, Jennings et al. 1999, Ditengou, Teale et al. 2008). In the absence of environmental heterogeneity, the endogenous LR spacing mechanism becomes dominant, and results in a relatively regular distribution of LRs along the primary root. The accumulation of the plant hormone auxin plays a central role in LR initiation and its subsequent development. The position of newly formed LRs is instructed by the frequency and amplitude of an oscillating auxin maximum near the root elongation zone. This oscillation is in turn controlled by a complex interplay between specific carotenoid-derived signals, programmed cell death of the lateral root cap, and proliferation patterns in the meristem (Moreno-Risueno, Van Norman et al. 2010, Xuan, Band et al. 2016, van den Berg, Yalamanchili et al. 2021).

Adventitious roots (AR) represent a third type of roots, which depending on the species and their position on the plant can play diverse functions like anchorage and support, vegetative propagation, increasing the mineral uptake from topsoil, or replacing a damaged primary root. The capacity of forming de novo roots on the aboveground organs is pivotal for the clonal propagation of elite varieties and hence the strong interest of agroindustry in methods that stimulate adventitious rooting. Wounding and incubation in the dark are commonly applied treatments to stimulate AR formation in vegetative propagated food, ornamental and medicinal crops (Giovannelli and Giannini 2000, Xiao, Ji et al. 2014). By default, *Arabidopsis* does not develop ARs and only generates them after excision of the main root system or when strongly etiolated after a dark period, which resulted in two approaches for studying AR (Smith and Fedoroff 1995, Sorin, Bussell et al. 2005). The cutting of the main root system leads to a local auxin accumulation near the wounding site, which together with wounding associated signals induces AR formation (De Klerk, Van Der Krieken et al. 1999). The second approach is based on exposure of etiolated Arabidopsis hypocotyls to light that is known to induce AR (Takahashi, Sato-Nara et al. 2003; Zeng, Schotte et al. 2022). Like

embryonic root and LR specification, both AR induction systems rely on the modulation of the plant hormone auxin. Auxin accumulation in the pericycle of the *Arabidopsis* hypocotyl results in AR initiation, and the subsequent AR development and emergence are expected to follow an LR-related mechanism (Welander, Geier et al. 2014). This is supported by the emerging framework for AR-associated auxin signalling and downstream transcriptional responses (Bellini, Pacurar et al. 2014, Welander, Geier et al. 2014, Lakehal, Chaabouni et al. 2019). However, in contrast to LR formation developmental processes, the mechanisms controlling auxin-induced AR formation remain poorly understood.

The endogenous auxin, indole-3-acetic acid (IAA) is a very potent molecule that shows little impact when applied exogenously because of chemical instability in light and rapid metabolic inactivation (Nissen and Sutter 1990). Indole-3-butyric acid (IBA) is more stable and slowly converted to IAA via beta-oxidation in specific tissues leading to LR and AR induction (De Rybel, Audenaert et al. 2012). To by-pass the stability issues, a wide variety of synthetic auxin analogues, agonists and pro-auxins have been developed (Ma, Grones et al. 2017, Todd, Figueiredo et al. 2020). Auxinic molecules fused to a hydrolysable amide bond such as indole acetamide, and different pro-auxins have more subtle auxinic effects (Savaldi-Goldstein, Baiga et al. 2008, Kerchev, MÜHlenbock et al. 2015, Gao, Dai et al. 2020) and some auxin analogues induce selective auxin responses and omit undesired effects (Vain, Raggi et al. 2019).

While commonly used synthetic auxins like 1-naphtaleneacetic acid (NAA), 2,4-dichlorphenoxyacetic acid (2,4-D) and 2-methyl-4-chlorophenoxyacetic acid (MCPA) display strong effects, their poor transport properties preclude the establishment of morphogenic hormone gradients and regular organogenesis patterns. Such undesired effects are not observed with auxinic molecules that are converted within the plant, such as IBA, that is for almost 90 years commonly applied for adventitious rooting (Zimmerman 1935). Here, we identified a new auxin agonist, named HYSPARIN (HYS), that strongly induces hypocotyl adventitious rooting and does not induce lateral roots. We show that it does not act as the typical synthetic auxin as it does not inhibit primary root growth nor activate rapid auxin responses. Yet, its adventitious rooting activity completely depends on canonical auxin signalling and partially on the TMK-mediated auxin signalling (Xu, Dai et al. 2014, Friml, Gallei et al. 2022). Using HYS, we demonstrate that transcriptome changes associated with early adventitious rooting largely overlap with that of LR development and that members of the SAUR19 subfamily, OFP transcription factors and AGC kinase act as negative regulators of AR formation. Importantly, HYS not only induces hypocotyl AR

formation in Arabidopsis, but also in tomato hypocotyls and rice, indicating that its bioactivity involves an evolutionary conserved AR signalling mechanism.

Results

Small molecules selectively inducing adventitious rooting in hypocotyls

After etiolation, *Arabidopsis* hypocotyls form only 1-5 ARs, a response that is strongly increased by synthetic auxins such as 1-NAA (Supplementary Fig. S1a, b). Typical synthetic auxins enhance, in addition to AR formation, also LR induction, and strongly inhibit primary root tip growth (Supplementary Fig. S1c, d). To decorticate AR formation signalling elements distinct from those regulating LR induction, we performed a screen for AR-selective auxin-like compounds. A compilation of 87 small molecules previously identified in a chemical genetics screen as activators of root pericycle cell division (DIVERSet^{TM} ChemBridge Crop) (De Rybel, Audenaert et al. 2012) were tested for their capacity to induce ARs in de-etiolated seedlings (Supplementary Fig. S1e). A distinction was made between emerged ARs and non-emerged AR primordia (ARP), which are visualized inside the hypocotyl at low magnification (Zeng, Schotte et al. 2022). We also quantified the number of emerged LR and non-emerged LR primordia (LRP) based on similar classification criteria. All compounds that induced AR, ARP, LR or LRPs to levels above those of control were retained and analysed via hierarchical clustering. The compounds were grouped according to preferential activities towards inducing ARP + LRP (I), AR (II), AR + LR (III), and LR+LRP formation (IV). Three molecules (C77, C76, C54) grouped in the AR- specific activity cluster II (Fig. 1b). The classic auxins IAA, IBA, 2,4-D and 1-NAA (hereafter NAA) grouped in the clusters I, III, and IV, in line with their respective capacity to induce LR organogenesis (Fig. 1a; Supplementary Table S1). The bioactivity of the three lead compounds was validated at 1, 10 and 50 μM (Fig. 1c-f). The AR phenotype was saturated at 1 μM for all three molecules while C76 and C77 showed a reduced rooting response at 50 μM, by and large compensated for by a strong increase of ARP. Compound C54 strongly induced AR production and inhibited LR formation at each concentration. Strikingly, seedlings treated with compounds C76 and C77 had a very short primary roots and leaf development was strongly impaired (Fig. 1b; Supplementary Fig.1f). In contrast, C54 had much milder effects on primary root length and leaf development (Fig. 1b; Supplementary Fig.1f). This macroscopic phenotypic assessment identified C54 as a unique compound, specifically activating

AR formation in hypocotyls. Therefore, C54 was selected for further characterization, and was renamed Hypocotyl-specific Adventitious Root Inducer (HYSPARIN; HYS).

HYSPARIN potently induces AR formation in tomato and rice

In tomato hypocotyls and stems, AR arise respectively from phloem-associated cambial cells (Alaguero‐Cordovilla, Sánchez‐García et al. 2021), and from differentiated primary phloem parenchyma cells, respectively (Omary, Gil-Yarom et al. 2022). In rice, adventitious (nodal) roots originate from ground meristem cells adjacent to the peripheral cylinder of vascular bundles in the stem (Itoh, Nonomura et al. 2005). Therefore, we asked if HYS rooting activities would be conserved in species in which ARs do not arise from xylem-pole pericycle cells, which is the case in *Arabidopsis* hypocotyls.

First, we tested the capacity of HYS to induce AR on the hypocotyl of etiolated tomato cultivars Ailsa Craig, Rio Grande and Moneymaker. Rio Grande formed on average 0.3 ARs while the other two cultivars did not spontaneously form AR. HYS-treatment triggered AR formation in all tomato cultivars in a dose-dependent manner with 10 µM as the optimal concentration (Supplementary Fig. S2). As in *Arabidopsis*, HYS treatment did not have strong effects on primary root growth and LR development in tomato (Fig. 2a, Supplementary Fig. S2). Next, we investigated the application of HYS on tomato in green house conditions for inducing root formation. Four-day-old tomato seedlings sprayed with 10 µM HYS formed more ARP compared to the mock treated plants (Fig. 2b, c).

Next, we tested the monocot model plant *Oryza sativa*. Four-day old rice seedlings were cultured in the presence of different concentrations of NAA or HYS and primary root length and ARs were quantified. Primary root growth was inhibited by NAA whereas HYS did not (Fig. 2d). Strikingly, rice plants sprayed with HYS produced about 25% more roots than the mock-treated plants (Fig. 2e, f). Jointly, these data demonstrated that HYS is a potent inducer of AR in shoot-derived tissues of evolutionarily diverse species with different root developmental programs.

AR formation depends on TIR1/AFB and TMK auxin signalling

As AR involves canonical auxin signalling with the stabilisation of TIR1/AFB-Aux/IAA interaction, for Aux/IAA proteasomal degradation and derepression of ARF transcription factors (Lakehal and Bellini 2019, Mhimdi and Pérez-Pérez 2020), a set of key auxin signalling mutants were screened for HYS-resistant AR formation. The *tir1-1* single, the *tir1-1afb2-3* double and *tir1-1afb2-3,3-4 triple* mutant displayed increasingly stronger resistance to HYS-induced AR formation (Fig. 3a, b; Supplementary Fig.3 a, b). In contrast, the *afb2* and *afb3* single mutants responded to HYS as WT (Fig. 3a, b; Supplementary Fig.3a, b). Among the dominant negative *Aux/IAA* mutants, there was strong HYS resistance in *axr5-1*, *slr-1*, *axr2-1*, but not in *iaa28-1* and *msg2-1* (Fig. 3a, b; Supplementary Fig.3 a, b). HYS-induced AR formation was severely impaired in *arf10-2arf16-2* and *nph4-1arf19-1* double mutants, but not in *arf7/nph4-1* and *arf19-1* single mutants (Fig. 3 a, b).
Lastly, we evaluated the genetic involvement of the TMKs, that represent a plasma membrane localised auxin perception mechanism (Xu, Dai et al. 2014). All single mutants displayed moderate to strong HYS resistance, with *tmk1,4* double mutants showing the strongest reduction in HYS-induced AR formation (Fig. 3c, d; Supplementary Fig.3 e, f). The hypocotyl tissue in *tmk1,4* was packed with proliferating cells, suggesting that TMKs do not control HYS-induced proliferation in the hypocotyl (Fig. 3c). The defect in AR morphogenesis, could reflect a role in cell division orientation alike the one described for LR morphogenesis (Huang, Zheng et al. 2019). Jointly, these data demonstrate that HYS-induced AR formation requires canonical auxin signalling, suggesting that HYS converges directly or indirectly on auxin signalling and/or distribution and thus mimics auxin agonist activity.

HYS does not act as a classical auxin

Next, we characterized HYS activity in comparison with the commonly used synthetic auxin NAA. A dose-response experiment showed that the near-maximal AR-inducing activity of HYS was reached at 0.05 µM, while the lowest AR-inductive concentration of NAA was 100-fold higher (Fig. 4a). HYS and NAA had an opposite effect on primary root growth whereby HYS stimulated growth over a concentration range of three orders of magnitude (0.05 - 50 µM) and NAA strongly inhibited root growth already at 0.05 µM (Fig. 4b). For comparison, endogenous auxin IAA inhibits root elongation at the nM range (Fendrych, Akhmanova et al. 2018, Li, Verstraeten et al. 2021). The strong effect of NAA on root growth has been associated with the capacity to strongly induce expression of the

auxin signalling reporter *proDR5::GUS*. NAA induced *proDR5::GUS* expression along the hypocotyl within 4h, while HYS did not within the same time frame (Fig. 4c; Supplementary Fig. S4a). Moreover, in contrast to NAA, HYS had no impact on the stability of DII-VENUS, a reporter for TIR1/AFB-mediated auxin signalling (Fig. 4d; Supplementary Fig. S4b). Auxin induces CNGC14-mediated Ca^{2+} signals downstream of TIR1/AFB auxin co-receptors (Dindas, Scherzer et al. 2018). Application of IAA to Arabidopsis seedlings expressing the sensitive genetically encoded calcium reporters R-GECO1 or YC-Nano65 (Horikawa, Yamada et al. 2010, Zhao, Araki et al. 2011), induced a strong Ca^{2+} response. In contrast, HYS treatment did not elicit any Ca^{2+} responses using either reporter (Fig. 4e, f; Supplementary Fig. S4c-e). The inability to elicit any TIR1/AFB-dependent response indicated that HYS does not interact with TIR1/AFB co-receptors. To test this hypothesis, surface plasmon resonance (SPR) assays were performed. HYS did not bind to the auxin co-receptor TIR1 nor did it competitively inhibit the binding of IAA (Supplementary Fig. 4g, h). While HYS induces AR it defies the concept of classic auxin agonists altering the expression of the markers *proDR5::GUS* and DII-VENUS and inducing rapid Ca^{2+} signalling upon binding TIR1/AFB co-receptors. To gain unbiased insight into the early transcriptional responses, we analyzed the transcriptome of seedlings treated with HYS and NAA. Within 30min, NAA triggered strong differential expression of 272 transcripts relative to the mock treatment (FDR ≤ 0.5; Supplementary Fig. 4f, g). As expected, this short auxin treatment induced the expression of multiple primary auxin-responsive genes (Supplementary Table S2). In contrast, only 4 transcripts were differentially regulated by HYS treatment in comparison to the mock. Interestingly, each of these transcripts was also differentially regulated by NAA (Supplementary Fig. 4g). These data further corroborated that HYS does not induce AR formation through direct, rapid effects on TIR1/AFB mediated auxin signalling and indicates that HYS stimulates AR formation indirectly, while depending on the canonical auxin signaling pathway.

Histology of HYS-induced AR development

Given that HYS strongly induces AR without inducing LR, it allows dissecting early molecular signalling during adventitious rooting. First, we characterized the origin of HYS-induced ARs. At the morphological level, HYS-induced AR initiation can be recognized by anticlinal cell divisions in the hypocotyl pericycle (stage I), followed by periclinal cell divisions giving rise to a stage II primordium, and subsequent cell divisions that gradually develop into a functional AR primordium (Fig. 5a). No

cell divisions were observed in the endodermis, cortex or epidermis indicating that HYS induces AR formation following endogenous AR morphogenesis and development (Della Rovere, Fattorini et al. 2013). Next, we set-up to outline the HYS response by monitoring the HYS-induced ARP induction over time, based on histologically recognizable AR events. Up to 20h after treatment, ARPs were occasionally observed with the number of ARPs strongly increasing after 24h, reaching saturation after 36-40h of treatment (Fig. 5b). Over this time-course, the initial increase in ARP was followed by a gradual increase of older developmental stages at the expense of younger stages (Supplemental Fig. 5a-j). Plotting the position of the different developmental stages along the hypocotyl at 40 h of HYS treatment showed a relative random pattern of the different stages with the youngest developmental stages at the upper and lower edges of the AR zone (Fig. 5c), indicating that HYS induces AR formation relatively synchronously across a large area, with its activity tapering off to the shootward and rootward edges of this region (Supplemental Fig. 5k).

To map key molecular events in the HYS response, we used reporters for important aspects of the early stages of AR development. As a marker for proliferation, the G2/M cell cycle reporter *proCYCB1;1::GUS* (Himanen, Boucheron et al. 2002) revealed initiation of cell divisions after 24h, followed by divisions in the upper two thirds of the hypocotyl after 48h (Fig. 5d). The auxin response marker *proDR5::GUS* was also prominently induced in this area after 24h, suggesting that HYS activates a transcriptional auxin response only after 24h (Fig. 5e). Notably, *proDR5::GUS* activity was not restricted to the pericycle, but was also induced in the endodermis, cortex and epidermis of the hypocotyl (Fig. 5e).

HYS dependent gene expression during AR induction and development

Our time-course histological and marker analyses revealed the activation of cell proliferation in the hypocotyl pericycle within 24 h (Fig. 5), suggesting that the earliest HYS signals, and thus early AR induction events, occurs just prior to this timing. Therefore, we selected three time points to capture the onset of HYS dependent gene expression during AR-induction. Three-day-old, etiolated WT (Col-0) seedlings were transferred to new medium with or without HYS 10 µM and exposed to light for 16, 20 and 24 hours. A control of corresponding untreated etiolated samples at 0 h was included in the analysis. Compared to the untreated control at 0 h, numerous genes related to light signalling and photomorphogenesis were differentially regulated in mock-treated samples after 16 h, 20 h and 24 h, reflecting the light response (Supplementary Table S3). Using an ANOVA-like quasi-likelihood F-test in EdgeR, we identified 631 genes that were differentially expressed upon

HYS treatment after 16 h, 20 h and/or 24 h (FDR<0.05). Subsequent hierarchical clustering of differentially expressed genes (DEGs) based on log_2-fold changes compared to the corresponding mock-treated samples revealed roughly four categories of HYS-induced gene expression patterns (Fig. 6a).

The bulk of genes was transcriptionally induced relative to the mock treatment, with few genes being downregulated. The up-regulated genes were strongly enriched for auxin-related gene functions, such as gravitropism, auxin homeostasis, auxin-activated signalling, auxin transport and (lateral) root morphogenesis (Fig. 6a; Supplementary Table S3). The downregulated genes were enriched for genes associated with RNA metabolism and translation (Fig. 6a; Supplementary Table S3). Interestingly, several cytokinin signalling components were downregulated, which is consistent with auxin-cytokinin antagonism during AR formation. Enriched functionalities in the HYS-induced gene lists indicate that HYS-induced AR formation is similar to LR formation. Accordingly, when we analysed the behaviour of HYS-regulated genes in LR initiation transcriptomes, we found substantial overlap with genes associated with auxin-induced LR development, including multiple key regulators of LR initiation (*LBD18, LBD29, GATA23, MAKR4*) and emergence (*SHY2/IAA3, HAESA*). Consistent with the transcriptome data, reporters for early LR initiation markers (*proMAKR4::GUS, proIAA2::GUS, proPUCHI::GUS* and *proGATA23::GUS*) were induced by HYS in the hypocotyl around the same time as *proDR5::GUS* activity (Fig. 6b-d; Supplementary Fig. 6a-d). Expression of the LR initiation markers in the roots was not affected by HYS, in agreement with the hypocotyl specific activity of HYS (Supplementary Fig. S6e). To determine whether HYS mediated induction of gene expression was dependent on canonical auxin signalling, the expression levels of HYS responsive auxin related genes (SAUR23, IAA6, PIN3, GH3-3, ARGOS, and RTFL13) was analysed by Q-PCR. Their expression was enhanced by HYS in Col-0 and not in the arf7-arf19 auxin response mutant, except for GH3.3 that was induced to about half of the level recorded for Col-0 (Fig. 6e). Together, these results show that HYS mediated gene expression depends on ARF auxin signalling and primarily regulates expression in the hypocotyl, in agreement with its capacity to induce hypocotyl AR. Further mechanistic overlap with LR development is apparent from the HYS-resistant AR induction in LR-defective auxin signalling mutants, such as *tir1afb2afb3* and *arf7arf19* (Fig. 3).

In the root, *SHY2/IAA3* is specifically expressed in the endodermis, where it controls auxin signalling for LR emergence and initiation (Vermeer, von Wangenheim et al. 2014). Similarly to the *shy2-2* LR phenotype, inhibition of auxin signalling in the endodermis by overexpressing a stabilized version

of SLR/IAA14 (mIAA14) in the endodermis *(proSCR::mIAA14-GR*) strongly impaired the formation of emerged AR in HYS treated plants (Supplementary Fig. 6 f, g). In these conditions, HYS induced massive proliferation in internal tissues of the hypocotyl, reminiscent of the LR emergence defect described for *shy2-2* mutants (Supplementary Fig. 6 g). The HYS induced expression of *SHY2/IAA3* in our transcriptome data was validated using *proSHY2::NLS-3xmVenus*. Instead of the endodermis-specific expression seen in the root, *proSHY2::NLS-3xmVenus* was active and induced in all tissues of the hypocotyl, including the pericycle (Fig. 6e, f). Consistently with inhibition of auxin signalling within this expression domain beyond the endodermis, *shy2-2* was completely HYS resistant, as indicated by a lack of pericycle proliferation (Fig. 6 h,i).

Collectively, the data illustrate a strong similarity in gene regulation between HYS-activated AR formation and LR formation.

To explore genes specifically involved in AR formation, we examined the HYS induced genes that were not identified in LR transcriptome analyses (Supplementary Table S4). From these genes we selected a set of SAUR19 subfamily genes that are known to be primarily expressed in hypocotyls (*SAUR19, SAUR20, SAUR21, SAUR22, SAUR24, SAUR26, SAUR29, SAUR62*) (Spartz, Lee et al. 2012, Sun, Wang et al. 2016, Wang, Yu et al. 2020). The reporter *proSAUR24::GFP* corroborated the HYS inducibility of *SAUR24* (Fig. 7a). Then, we investigated it relevance for HYS induced AR responses, using a SAUR19 overexpression line (*pro35S::SAUR19*; (Spartz, Lee et al. 2012)) and *saur19/20/21/22/23/24* sextuple mutant (Wang, Yu et al. 2020). Consistently with these SAURs controlling HYS-induced AR formation, we found that the *SAUR19* overexpressor displayed strong resistance to HYS-induced AR formation (Fig. 7b, c). The *35S::SAUR19* had more AR than wild type in the DMSO control (Supplementary Fig. 7a, b), possibly due to effects on auxin transport in etiolated hypocotyls (Spartz, Lee et al. 2012). Also, HYS induced more AR in the *saur19/20/21/22/23/24* sextuple mutant than in the wild type (Fig.7b, c; Supplementary Fig. S7a, b). Jointly, these data illustrate that SAUR19 subfamily genes are negative regulators of HYS-induced AR formation.

Next, we selected the AGCVIII kinases family members AGC1 kinase12 (AGC1-12)_that has been shown to phosphorylate the auxin transporter PIN1 (Haga, Frank et al. 2018) and AGC2 kinase 3/UNICORN (AGC2-3/UNC) (Enugutti, Kirchhelle et al. 2012) that controls planar organ growth (Scholz, Pleßmann et al. 2019). So far neither kinase has been linked to root branching. The HYS-

induced expression of *AGC1-12* and *AGC2-3* after 16h and 24h HYS treatment was confirmed by Q-RT-PCR (Fig. S7c, d). Importantly, HYS AR induction is impaired in the *agc2-3* mutant and not in the *agc1-12* mutant (Fig. 7d, e), identifying that AGC2-3 is more critical for AR formation.

OVATE FAMILY PROTEINS (OFPs) were proposed to function as transcriptional repressors regulating plant growth and development (Wang, Chang et al. 2007, Li, Wang et al. 2011, Wang, Chang et al. 2011). Furthermore, OFPs expression is involved in feedback phytohormone signalling and biosynthesis pathways within the developing organ (Yang, Shen et al. 2016, Wang, Clevenger et al. 2019, Snouffer, Kraus et al. 2020). No differences in HYS-induced AR formation were evident in *ofp4-2* and double *ofp1-1ofp4-2* relative to the wild type. In the triple mutant *ofp1-1/3-1/4-2* and *ofp1-1/3-1/5-1* we observed an increased HYS-induced AR formation. The spatial distribution of HYS-induced ARs revealed that the AR increase in the mutant is associated with expanding the AR-forming zone of the hypocotyl towards the shoot apical meristem. In contrast, overexpression *OFP4* led to a significant reduction in HYS-sensitive AR formation (Fig. 7f, g). Collectively, these data identify SAURs, OPFs as negative regulators and AGC2-3 as a positive regulator of HYS-activated AR formation.

Discussion

Hypocotyl-specific auxin activity of HYS

Nearly all aspects of plant development are under control of auxin. In the root, it triggers lateral root initiation, morphogenesis and emergence, regulates cell elongation, root meristem activity, and root hair development (Vanneste and Friml 2009, Overvoorde, Fukaki et al. 2010). Here, we identified HYSPARIN a chemical that activates AR formation in *Arabidopsis,* tomato and rice. The induction of AR by HYS is strongly dependent on canonical auxin signalling, as seen by the strong HYS resistance of multiple mutants defective in this pathway. This is further corroborated by the activation of the auxin response reporter *proDR5::GUS*, as well as by the induction of typical auxin responsive genes such as *SAUR*s, *Aux/IAA*s and *GH3*s. However, in striking contrast to NAA, HYS suppresses LR development and stimulates primary root growth. This is reflected by its inability to induce *proDR5::GUS* or induce DII-VENUS degradation in the root, or to bind TIR1. An important feature of the HYS-induced auxin responses and AR formation is that it is much delayed compared to auxin analogues. The induction of *proDR5::GUS* activity in the hypocotyl requires more than 12h,

and after a 30 min treatment, nearly no transcriptional changes have been detected which may be related to slow uptake of the molecule or indirect activation of auxin signalling.

Pro-auxins release bioactive auxins upon in planta hydrolysis of the amide bond that keeps these molecules inactive. HYS contains a similar amide bond, suggesting that it could also be activated by hydrolysis. However, the hydrolysis of none of the reported pro-auxins does seems to be tissue-specific as seen by strong induction of auxin responses not only in the hypocotyl, but also in the root (Savaldi-Goldstein, Baiga et al. 2008, Kerchev, MÜHlenbock et al. 2015). Therefore, HYS is selectively metabolized in the shoot or alternatively HYS-AR bioactivity involves an independent mechanism that operates in the shoot.

Auxin-induced AR development is reminiscent to auxin-induced LR development

The analogous anatomy of LRs and ARs hints to a conserved developmental programme for both root types. However, an angiosperm-specific subclade of LOB DOMAIN (LBD) transcription factors was identified in which different subclasses attained root-type specific specialization (Omary, Gil-Yarom et al. 2022), illustrating fundamental differences between LR and AR development. Our analysis on HYS-induced AR formation revealed an important overlap of the transcriptomes of auxin responsive LR and AR associated transcriptomes. This includes the core auxin signalling machinery governed by TIR1, AFB2, AFB3, SLR/IAA14, AXR5/IAA1 regulating the activities of ARF7 and ARF19 transcription factors. However, in contrast to its strong LR defect (Rogg, Lasswell et al. 2001), *iaa28-1* did not show strong AR defects emphasizing differences also in auxin signalling between the two root types. The inverse situation was true for *axr2-1/iaa7* which has a normal LR density (Nagpal, Walker et al. 2000), but a strong HYS-resistant AR development. Also the strong AR defect in *shy2-2/iaa3* was distinct from the reported LR phenotype that is mainly characterized by a defect in the LR emergence and morphogenesis (Vermeer, von Wangenheim et al. 2014). These phenotypic differences likely reflect shifts in the expression domain of these dominant negative Aux/IAAs between shoots and roots.

The case of *shy2-2/iaa3* is interesting, as its LR defect is largely due to the inhibition of auxin signalling in the endodermis rather than the pericycle. Based on this observation, local auxin signalling in the endodermis is important for spatial accommodation of incipient LR primordia, still allowing auxin-induced LR initiation (Vermeer, von Wangenheim et al. 2014). We found a similar importance for auxin signalling in the endodermis regulating AR emergence by endodermis-specific expression of a dominant negative mIAA14. This, together with the induced expression of the cell

separation regulator HAESA, strongly suggest that AR and LR emergence employ similar mechanisms.

The current molecular framework for AR formation was largely established based on mutants with altered AR capacity. The key role for auxin was established by the characterisation of *superroot* (*sur*) mutants in which auxin overproduction causes hyperproliferation of AR. Suppressor screens in the *sur2-1* mutant background identified multiple genes involved in auxin biosynthesis (ASA1/WEI2, ASB1/WEI7, TSB1) and signalling (AXR1, ALF4, RCE1 and SHY2/IAA3), supporting a central role for auxin in AR formation (Pacurar, Pacurar et al. 2014). A directed mutant analysis implicated TIR1 and AFB2, together with IAA6, IAA9 and IAA17 as major components of AR-associated auxin perception (Lakehal, Chaabouni et al. 2019). This auxin signalling module was proposed to control the expression of IAA and JA conjugating GH3s (GH3.3, GH3.5 and GH3.6) via ARF6, ARF8 and ARF17 (Gutierrez, Mongelard et al. 2012, Lakehal, Chaabouni et al. 2019). The induction of these GH3s stimulate AR initiation by lowering the pool of free JA (Gutierrez, Mongelard et al. 2012). Additionally, ARF7 and ARF19 have been shown to contribute to AR formation through the induction of LBD transcription factors (Lee, Cho et al. 2019), which have key functions in LR and AR initiation (Omary, Gil-Yarom et al. 2022). We found that HYS-induced AR formation depends largely on the outlined molecular framework of auxin-induced AR formation, highlighting HYS as a very useful tool to study AR formation.

HYS specific regulators of AR formation

Many of the HYS-responsive genes were not detected in the LR developmental program reflecting the different contexts in which LR and AR are induced. Here, we identified three gene subfamilies SAUR19, OFP and AGCVIII kinases as HYS-specific regulators of AR induction. Enhanced expression of SAUR genes has been associated with either more root branching in *Arabidopsis* (Kong, Zhu et al. 2013), in rice (Park, Kim et al. 2021) and *Medicago* (Cheng, Gou et al. 2017) or with reduced root branching, also in rice (Kant, Bi et al. 2009). In general, Arabidopsis SAUR proteins promote cell expansion. The suppression of AR development by SAUR19-24 subfamily members is consistent with the interference of cell expansion and the initiation of new root meristems. Paradoxically, SAUR expression is enhanced by HYS, suggesting a more complex relation between these two processes.

AGCVIII kinases, with PINOID/PID as the founder of this family in plants, have been proposed to be evolutionary derived from an ancestral phototropin regulating PIN auxin transporters (Galván-Ampudia and Offringa 2007). The AGCVIII kinases D6 PROTEIN KINASE (D6PK), PID directly regulate PIN-mediated auxin transport by phosphorylation of the hypocotyl expressed PIN3, PIN4, and PIN7 to control phototropic hypocotyl bending and WAG2 controls root waving through PIN3 (Santner and Watson 2006, Willige, Ahlers et al. 2013, Haga, Hayashi et al. 2014, Zourelidou, Absmanner et al. 2014, Grones, Abas et al. 2018). In contrast to these AGCVIII kinases, AGC2-3/UNICORN kinase regulates planar growth development by attenuating the transcription factor ATS and AGCVIII kinase PDK1 (Enugutti, Kirchhelle et al. 2012, Scholz, Pleßmann et al. 2019). Our results indicate that UNC, perhaps in a redundant manner with AGC1-12, is involved in controlling AR induction, expanding the role of these kinases in plant development.

The OVATE FAMILY PROTEINS are transcriptional inhibitors that bind to the cytoskeleton and regulate many aspects of plant growth and development and secondary cell wall synthesis (Pagnussat, Yu et al. 2007, Li, Wang et al. 2011, Liu and Douglas 2015). While a role in controlling fruit shape seems conserved in many fruit crops, the functional characterization is complicated by the redundancy of OFPs (van der Knaap, Chakrabarti et al. 2014). The role of OFPs in plant development must be broader because of their impact on abscisic acid, gibberellin, auxin, and brassinosteroid signalling. In rice for instance, OsOFP6 was shown to alter the shape and size of rice grains and to modulate the length of lateral roots presumably through regulation of auxin transport (Ma, Yang et al. 2017). In Arabidopsis, root growth in early seedlings is controlled in an ABA dependent manner by AtOFP1. These studies together with the role in AR induction show that different members of the OFP family regulate root growth and root branching. OFPs do not contain a DNA binding domain and therefore are likely influencing root development via the interaction with TALE (three amino acid loop extension) homeodomain transcription factors such as KNAT3 and KNAT7 that regulate secondary cell wall formation (Li, Wang et al. 2011, Wang, Yamaguchi et al. 2020). Our transcriptome data show an upregulation of *KNAT7* by HYS suggesting that this family member may function as a co-regulator of OFPs in adventitious rooting, perhaps analogous to KNAT6 that was shown to control LR development (Dean, Casson et al. 2004).

A conserved adventitious and lateral root signalling pathway

A recent study in tomato identified SHOOT BORNE ROOTLESS (SBRL), a LATERAL ORGAN BOUNDARIES DOMAIN (LBD) transcription factor expressed in a small population of primary phloem-associated cells that generate the initials of adventitious root primordia (Omary, Gil-Yarom et al. 2022). SBRL, like the other LBD IIIB subclass members RTCS in maize, and CRL1 in rice, is essential for shoot-borne root formation, while members of the subclass IIIA are critically important for LR formation (Omary, Gil-Yarom et al. 2022). In Arabidopsis, LR and AR formation depend on LBD16 and an evolutionary conserved subset of LBD transcription factors (LBD29 and LBD18 respectively (Okushima, Fukaki et al. 2007, Lee, Cho et al. 2019). These LBDs are under control of specific AUX/IAA ARF auxin modules that we here show to display substantial overlap in downstream transcriptional regulation. The strong conservation of the molecular elements implies that LR and AR initiation is evolutionary conserved and involves only a limited number of root specific factors that are recruited to either AR or LR development via root-type specific upstream regulatory elements.

Materials and Methods

Plant material

The *tir1-1* (Ruegger, Dewey et al. 1998), *afb2-3* (Parry, Calderon-Villalobos et al. 2009), *afb3-4* (Parry, Calderon-Villalobos et al. 2009), double *tir1-1afb2-3* (Parry, Calderon-Villalobos et al. 2009), triple *tir1-1afb2-3afb3-4* (Parry, Calderon-Villalobos et al. 2009), *axr5-1/iaa1* (Yang, Lee et al. 2004), *axr2-1/iaa7* (Wilson, Pickett et al. 1990), *slr-1/iaa14* (Fukaki, Tameda et al. 2002), *msg2-1/iaa19* (Tatematsu, Kumagai et al. 2004), *iaa28-1* (Rogg, Lasswell et al. 2001, Rinaldi, Liu et al. 2012), *arf7/nph4-1* (Harper, Stowe-Evans et al. 2000), *arf19-1* (Okushima, Overvoorde et al. 2005), double *arf7-1arf19-1* (Okushima, Overvoorde et al. 2005), double *arf10-2arf16-2* (Wang, Wang et al. 2005), *tmk1-1* (SALK_016360) (Cao, Chen et al. 2019), *tmk2-1* (SAIL_1242_H07) (Cao, Chen et al. 2019), *tmk3-2* (SALK_107741) (Li, Verstraeten et al. 2021), *tmk4-1* (GABI_348E01) (Cao, Chen et al. 2019), double *tmk1-1tmk4-1* (Huang, Zheng et al. 2019), sextuple saur19/20/21/22/23/24 (Wang, Yu et al. 2020), *agc1-12* (FLAG_584B10), *agc2-3* (SALK_044862), *ofp4-2* (Li, Wang et al. 2011), double *ofp1-1ofp4-2* (Li, Wang et al. 2011), triple *ofp1-1/3-1/4-2* (a gift from Lacey Samuels) and triple *ofp1-1/3-1/5-1* (a gift from Lacey Samuels)mutants and overexpression line *35S::SAUR19* (Spartz, Lee et al. 2012), *35S::OFP4* (Li, Wang et al. 2011) used in this study are in the Columbia-0 (Col-0)

background. The *proSCR::miaa14-GR* was described previously (Fukaki, Nakao et al. 2005). The *shy2-2/iaa3 (Reed, Elumalai et al. 1998)* is in the Landsberg *erecta* (L*er*) background. The following GUS/GFP reporter transgenic plants were used in this study: *proDR5::GUS* (Ulmasov, Murfett et al. 1997), *proCYCB1;1::GUS* (Ferreira, Hemerly et al. 1994), *proMARK4::GUS* (Xuan, Audenaert et al. 2015), *proIAA2::GUS* (Luschnig, Gaxiola et al. 1998), *proPUCHI::GUS* (Hirota, Kato et al. 2007), *proGATA23::GUS* (De Rybel, Vassileva et al. 2010), *proOFP3::GUS* (gift from Lacey Samuels), *proSAUR24::GFP* (Wang, Yu et al. 2020), *SHY2pro::NLS-3xmVenus* X *LBD16pro::3xmCherry-SYP122* (Vermeer, von Wangenheim et al. 2014, Stöckle, Reyes-Hernández et al. 2022), *R-GECO1* (Zhao, Araki et al. 2011), *YC-Nano65* (Grenzi, Resentini et al. 2021), *DR5:Luciferase* (DR5:LUC) (Moreno-Risueno, Van Norman et al. 2010), *DR5:Luciferase X tir1-1afb2-3 (Xuan, Audenaert et al. 2015)* and *DII-VENUS* (Brunoud, Wells et al. 2012). Tomato [*lycopersicum cultivar* (cv) Ailsa Craig, Rio Grande and Moneymaker] seeds and Rice (*Oryza sativa*) were sterilized and transferred to petri dishes containing filter paper moistened with 10ml of distilled water and incubated in the dark for 3 days. After the emergence of the radicle, seedlings were transplanted to 10-liter soil pots for 2 days under low light condition before transferred in greenhouses.

Growth conditions and adventitious root phenotyping

Arabidopsis thaliana seeds were sterilized in chlorine gas in a closed desiccator for 4 hours. The surface sterilised seeds were sown on half-strength (0.5x) Murashige and Skoog (MS) medium supplemented with 0.5%(w/v) sucrose, 0.8%(w/v) agar and 0.05%(w/v) MES at pH 5.7. Plates with sterilized seeds were stratified at 4°C for 4 days in the dark. Following the vernalisation treatment, the plates were incubated in the light (22°C, 70 µmol /m²s) for 8h to stimulate germination before being incubated for 3 days in the dark to induce hypocotyl elongation. Well elongated seedlings were transferred to chemical treatments and ARs phenotype were evaluated after an additional 10 days in a growth chamber at 70% relative humidity and 22 °C, with 16 h/8 h light/dark cycles (70 µmol/m^2s). Stock solutions of all hormones and chemicals were dissolved in DMSO, which was used as mock treatment. Hormonal and chemical concentrations used were as indicated in the text.

Chemical treatments

For the chemical biology screen, a selection of 84 small molecules derived from a 10,000 diverse compounds library (DIVERSetTM ChemBridge Crop.) was tested for adventitious root induction in de-etiolated seedlings with 10µM concentration because of previously demonstrated impact on root development (De Rybel, Audenaert et al. 2012). Indole-3-acetic (IAA), 2,4-D and IBA were used

as a control because we reasoned that some of these molecules might also target the auxin signalling pathway. The roots (AR, ARP, LR and LRP) phenotype were inspected by a binocular Olympus SZX9. Stock solutions of the compounds used were dissolved at 10 mM in DMSO for all further experiments, and DMSO treatments were used in equal volume as solvent control. For the ChemBridge IDs and structures of chemical compounds, see Supplementary TableS1.

HYS synthesis

We synthesized HYS with confirmed chemical identities according to the protocol as described (Paczal, Bényei et al. 2006). The crystallisation of HYS was used for further experiments. See supplementary document for detailed experimental procedures.

Microscopy

For light microscopy, seedlings were cleared with methanol and NaOH and mounted as described (Malamy and Benfey 1997, Zeng, Schotte et al. 2022). The BX51 microscope (Olympus, Tokyo, Japan) equipped with differential interference contrast (DIC) optics were employed for inspect adventitious root primordia. The DII-VENUS fluorescence imaging was performed using Olympus IX-81 fluorescence microscope (Olympus, Tokyo, Japan).

Histochemical Analysis.

Arabidopsis seedlings were prefixed in ice-cold 90% (v/v) acetone for 30min to overnight at 4°C. The seedlings were then rinsed with NT buffer (100 mM Tris.HCl/50 mM NaCl, pH 7.0) and incubated in GUS reaction buffer (1ml 100 mM K3[Fe(CN)6] + 49 ml NT-buffer) for 30 min. Samples were transferred to fresh GUS staining solution: 0.25mM X-Gluc in GUS reaction buffer in the dark at 37 °C for 6-8 hours. The reaction was stopped by rinsing with NT-buffer for 1 hour, then seedlings were cleared as described and mounted in 50% Glycerol on a slide and imaged. Samples were observed using Olympus SZX9 and BX51 microscope (Olympus, Tokyo, Japan) for macro- and micro-images, respectively.

TIR1 Binding Activity Assay

TIR1 protein was purified using both His-trap and FLAG chromatography (Lee, Sundaram et al. 2014). A streptavidin-coated surface plasmon resonance (SPR) chip was coated with biotinylated peptides. Channels 2 and 3 were coated with the Aux/IAA7 degron sequence and the reference channel 1 was coated with biocytin (Quareshy, Uzunova et al. 2017). All the SPR assays were run

under standard conditions of 25 °C, flow rate 20 µL/min in HEPES-buffered saline with Tween 20 (20 mM Hepes, 150 mM NaCl, 3 mM EDTA + 0.01% Tween 20).

Ratiometric Ca2+ Imaging

Confocal microscopy Ca2+ imaging analyses as described (Pei, Liu et al. 2022). Arabidopsis roots were continuously perfused (0.9mL/min) in imaging solution (Behera, Xu et al. 2018). HYS (10 µM) or IAA (10 µM) treatment for 3 min was applied after 2 min. For wide-field Ca2+ analysis roots of pUBQ10-R-GECO1 pCaMV35S-YC-Nano65 lines were imaged in an inverted fluorescence Nikon microscope (Ti-E; http://www.nikon.com/) with a CFI Plan Apo VC 20X (N.A 0.75). Excitation was with a fluorescent lamp (Prior Lumen 200 PRO; Prior Scientific; http://www.prior.com) set to 30% with 561 nm (540/25 nm) for the R-GECO1, and 440 nm (436/20 nm) for YC-Nano65. R-GECO1 fluorescence emission was collected at 576–626 nm respectively. For the analysis of the YC-Nano65 line, the FRET CFP/YFP optical block A11400-03 (emission 1, 483/32 nm for ECFP; emission 2, 542/27 nm for FRET/Citrine) with a dichroic 510 nm mirror (Hamamatsu). Filters and dichroic mirrors were from Chroma Technology (http://www.chroma.com/). Ratio fluorescence images were quantified with Fiji (https://imagej.net/Fiji).

Acknowledgements

We thank M. Krebs (University of Heidelberg) for pUBQ10-R-GECO1; J. Kudla (University of Muenster) for pCaMV35S-YC-Nano65 Cameleon; J.E.M. Vermeer (University of Neuchâtel) for SHY2pro::NLS-3xmVenus X LBD16pro::3xmCherry-SYP122; L. Samuels (University of British Columbia) *ofp4-2, ofp1-1ofp4-2, ofp1-1ofp3-1ofp4-2, ofp1-1ofp3-1ofp5-1*, *35S::OFP4* and *proOFP3::GUS*; H. Chen (Peking University) for *saur19/20/21/22/23/24*, *35S::SAUR19 and proSAUR24::GFP Arabidopsis lines.*

This work was funded by Ghent University (BOF, 01SMO310 and 01J11415), Research Foundation Flanders (project 1S48517N and G094619N) and individual fellowships (SB-FWO, Sebastien Schotte 1S66418N; SB-FWO, Robin Lardon 1S48519N). Y.Z was supported by China Scholarship Council (CSC) (201806300036). H.K.T. was supported by a VIED scholarship.

Author contributions

D.G. proposed the initial idea with subsequent development by C.S., R.N., B.D.R., C.B., T.B., and S.V. D.G. and S.V. designed the study, Y.Z., I.V., H.K.T., S.S., D.O., T.H., M.Q., S.P.N., A.C., collected the data. D.G., S.V., and R.L. analysed the data. Y.Z, S.V., and D.G. prepared the first draft of the manuscript and all authors contributed significantly to subsequent revisions. Y.Z and I.V. contributed equally to this work.

Data availability

All data of this study are saved on a server of Ghent University and stored in accordance with a data management plan. Raw data are available from the corresponding author upon request.

Competing interests

None declared.

Material distribution

The author(s) responsible for distribution of materials integral to the findings presented in this article in accordance with the policy described in the Instructions for Authors (https://academic.oup.com/plcell/pages/General-Instructions) is: Danny Geelen (danny.geelen@ugent.be)

References

Alaguero‐Cordovilla, A., A. B. Sánchez‐García, S. Ibáñez, A. Albacete, A. Cano, M. Acosta and J. M. Pérez‐Pérez (2021). "An auxin‐mediated regulatory framework for wound‐induced adventitious root formation in tomato shoot explants." Plant, Cell & Environment **44**(5): 1642-1662.

Behera, S., Z. Xu, L. Luoni, M. C. Bonza, F. G. Doccula, M. I. De Michelis, R. J. Morris, M. Schwarzländer and A. Costa (2018). "Cellular Ca2+ signals generate defined pH signatures in plants." The Plant Cell **30**(11): 2704-2719.

Bellini, C., D. I. Pacurar and I. Perrone (2014). "Adventitious roots and lateral roots: similarities and differences." Annu Rev Plant Biol **65**(1): 639-666.

Brunoud, G., D. M. Wells, M. Oliva, A. Larrieu, V. Mirabet, A. H. Burrow, T. Beeckman, S. Kepinski, J. Traas and M. J. Bennett (2012). "A novel sensor to map auxin response and distribution at high spatio-temporal resolution." Nature **482**(7383): 103-106.

Cao, M., R. Chen, P. Li, Y. Yu, R. Zheng, D. Ge, W. Zheng, X. Wang, Y. Gu and Z. Gelová (2019). "TMK1-mediated auxin signalling regulates differential growth of the apical hook." Nature **568**(7751): 240-243.

Cheng, X., X. Gou, H. Yin, K. S. Mysore, J. Li and J. Wen (2017). "Functional characterisation of brassinosteroid receptor MtBRI1 in Medicago truncatula." Scientific Reports **7**(1): 9327.

De Klerk, G.-J., W. Van Der Krieken and J. C. de Jong (1999). "Review the formation of adventitious roots: new concepts, new possibilities." In Vitro Cellular & Developmental Biology-Plant **35**: 189-199.

De Rybel, B., D. Audenaert, W. Xuan, P. Overvoorde, L. C. Strader, S. Kepinski, R. Hoye, R. Brisbois, B. Parizot and S. Vanneste (2012). "A role for the root cap in root branching revealed by the non-auxin probe naxillin." Nature chemical biology **8**(9): 798-805.
De Rybel, B., V. Vassileva, B. Parizot, M. Demeulenaere, W. Grunewald, D. Audenaert, J. Van Campenhout, P. Overvoorde, L. Jansen and S. Vanneste (2010). "A novel aux/IAA28 signaling cascade activates GATA23-dependent specification of lateral root founder cell identity." Current Biology **20**(19): 1697-1706.
Dean, G., S. Casson and K. Lindsey (2004). "KNAT6 gene of Arabidopsis is expressed in roots and is required for correct lateral root formation." Plant molecular biology **54**: 71-84.
Della Rovere, F., L. Fattorini, S. D'angeli, A. Veloccia, G. Falasca and M. Altamura (2013). "Auxin and cytokinin control formation of the quiescent centre in the adventitious root apex of Arabidopsis." Annals of Botany **112**(7): 1395-1407.
Dindas, J., S. Scherzer, M. R. G. Roelfsema, K. von Meyer, H. M. Müller, K. Al-Rasheid, K. Palme, P. Dietrich, D. Becker and M. J. Bennett (2018). "AUX1-mediated root hair auxin influx governs SCFTIR1/AFB-type Ca2+ signaling." Nature communications **9**(1): 1174.
Ditengou, F. A., W. D. Teale, P. Kochersperger, K. A. Flittner, I. Kneuper, E. van der Graaff, H. Nziengui, F. Pinosa, X. Li and R. Nitschke (2008). "Mechanical induction of lateral root initiation in Arabidopsis thaliana." Proceedings of the National Academy of Sciences **105**(48): 18818-18823.
Enugutti, B., C. Kirchhelle, M. Oelschner, R. A. Torres Ruiz, I. Schliebner, D. Leister and K. Schneitz (2012). "Regulation of planar growth by the Arabidopsis AGC protein kinase UNICORN." Proceedings of the National Academy of Sciences **109**(37): 15060-15065.
Fendrych, M., M. Akhmanova, J. Merrin, M. Glanc, S. Hagihara, K. Takahashi, N. Uchida, K. U. Torii and J. Friml (2018). "Rapid and reversible root growth inhibition by TIR1 auxin signalling." Nature plants **4**(7): 453-459.
Ferreira, P., A. S. Hemerly, J. Engler, M. Van Montagu, G. Engler and D. Inzé (1994). "Developmental expression of the arabidopsis cyclin gene cyc1At." The Plant Cell **6**(12): 1763-1774.
Friml, J., M. Gallei, Z. Gelová, A. Johnson, E. Mazur, A. Monzer, L. Rodriguez, M. Roosjen, I. Verstraeten and B. D. Živanović (2022). "ABP1–TMK auxin perception for global phosphorylation and auxin canalization." Nature **609**(7927): 575-581.
Fukaki, H., Y. Nakao, Y. Okushima, A. Theologis and M. Tasaka (2005). "Tissue‐specific expression of stabilized SOLITARY‐ROOT/IAA14 alters lateral root development in Arabidopsis." The Plant Journal **44**(3): 382-395.
Fukaki, H., S. Tameda, H. Masuda and M. Tasaka (2002). "Lateral root formation is blocked by a gain‐of‐function mutation in the SOLITARY‐ROOT/IAA14 gene of Arabidopsis." The Plant Journal **29**(2): 153-168.
Galván-Ampudia, C. S. and R. Offringa (2007). "Plant evolution: AGC kinases tell the auxin tale." Trends in plant science **12**(12): 541-547.
Gao, Y., X. Dai, Y. Aoi, Y. Takebayashi, L. Yang, X. Guo, Q. Zeng, H. Yu, H. Kasahara and Y. Zhao (2020). "Two homologous INDOLE-3-ACETAMIDE (IAM) HYDROLASE genes are required for the auxin effects of IAM in Arabidopsis." Journal of genetics and genomics **47**(3): 157-165.
Giovannelli, A. and R. Giannini (2000). "Reinvigoration of mature chestnut (Castanea sativa) by repeated graftings and micropropagation." Tree Physiology **20**(18): 1243-1248.
Grenzi, M., F. Resentini, S. Vanneste, M. Zottini, A. Bassi and A. Costa (2021). "Illuminating the hidden world of calcium ions in plants with a universe of indicators." Plant Physiology **187**(2): 550-571.

Grones, P., M. Abas, J. Hajný, A. Jones, S. Waidmann, J. Kleine-Vehn and J. Friml (2018). "PID/WAG-mediated phosphorylation of the Arabidopsis PIN3 auxin transporter mediates polarity switches during gravitropism." Scientific Reports **8**(1): 10279.
Gutierrez, L., G. Mongelard, K. Flokova, D. I. Pacurar, O. Novak, P. Staswick, M. Kowalczyk, M. Pacurar, H. Demailly, G. Geiss and C. Bellini (2012). "Auxin controls Arabidopsis adventitious root initiation by regulating jasmonic acid homeostasis." Plant Cell **24**(6): 2515-2527.
Haga, K., L. Frank, T. Kimura, C. Schwechheimer and T. Sakai (2018). "Roles of AGCVIII kinases in the hypocotyl phototropism of Arabidopsis seedlings." Plant and Cell Physiology **59**(5): 1060-1071.
Haga, K., K.-i. Hayashi and T. Sakai (2014). "PINOID AGC kinases are necessary for phytochrome-mediated enhancement of hypocotyl phototropism in Arabidopsis." Plant physiology **166**(3): 1535-1545.
Harper, R. M., E. L. Stowe-Evans, D. R. Luesse, H. Muto, K. Tatematsu, M. K. Watahiki, K. Yamamoto and E. Liscum (2000). "The NPH4 locus encodes the auxin response factor ARF7, a conditional regulator of differential growth in aerial Arabidopsis tissue." The Plant Cell **12**(5): 757-770.
Himanen, K., E. Boucheron, S. Vanneste, J. de Almeida Engler, D. Inzé and T. Beeckman (2002). "Auxin-mediated cell cycle activation during early lateral root initiation." The Plant Cell **14**(10): 2339-2351.
Hirota, A., T. Kato, H. Fukaki, M. Aida and M. Tasaka (2007). "The auxin-regulated AP2/EREBP gene PUCHI is required for morphogenesis in the early lateral root primordium of Arabidopsis." The Plant Cell **19**(7): 2156-2168.
Horikawa, K., Y. Yamada, T. Matsuda, K. Kobayashi, M. Hashimoto, T. Matsu-ura, A. Miyawaki, T. Michikawa, K. Mikoshiba and T. Nagai (2010). "Spontaneous network activity visualized by ultrasensitive Ca2+ indicators, yellow Cameleon-Nano." Nature methods **7**(9): 729-732.
Huang, R., R. Zheng, J. He, Z. Zhou, J. Wang, Y. Xiong and T. Xu (2019). "Noncanonical auxin signaling regulates cell division pattern during lateral root development." Proceedings of the National Academy of Sciences **116**(42): 21285-21290.
Itoh, J.-I., K.-I. Nonomura, K. Ikeda, S. Yamaki, Y. Inukai, H. Yamagishi, H. Kitano and Y. Nagato (2005). "Rice plant development: from zygote to spikelet." Plant and cell physiology **46**(1): 23-47.
Kant, S., Y.-M. Bi, T. Zhu and S. J. Rothstein (2009). "SAUR39, a small auxin-up RNA gene, acts as a negative regulator of auxin synthesis and transport in rice." Plant physiology **151**(2): 691-701.
Kerchev, P., P. MÜHlenbock, J. Denecker, K. Morreel, F. A. Hoeberichts, K. Van Der Kelen, M. Vandorpe, L. Nguyen, D. Audenaert and F. Van Breusegem (2015). "Activation of auxin signalling counteracts photorespiratory H2O2 ‐ dependent cell death." Plant, cell & environment **38**(2): 253-265.
Kong, Y., Y. Zhu, C. Gao, W. She, W. Lin, Y. Chen, N. Han, H. Bian, M. Zhu and J. Wang (2013). "Tissue-specific expression of SMALL AUXIN UP RNA41 differentially regulates cell expansion and root meristem patterning in Arabidopsis." Plant and cell physiology **54**(4): 609-621.
Lakehal, A. and C. Bellini (2019). "Control of adventitious root formation: insights into synergistic and antagonistic hormonal interactions." Physiologia Plantarum **165**(1): 90-100.
Lakehal, A., S. Chaabouni, E. Cavel, R. Le Hir, A. Ranjan, Z. Raneshan, O. Novák, D. I. Păcurar, I. Perrone and F. Jobert (2019). "A molecular framework for the control of adventitious rooting by TIR1/AFB2-Aux/IAA-dependent auxin signaling in Arabidopsis." Molecular plant **12**(11): 1499-1514.
Lee, H. W., C. Cho, S. K. Pandey, Y. Park, M.-J. Kim and J. Kim (2019). "LBD16 and LBD18 acting downstream of ARF7 and ARF19 are involved in adventitious root formation in Arabidopsis." BMC Plant Biology **19**(1): 1-11.

Lee, H. W., C. Cho, S. K. Pandey, Y. Park, M. J. Kim and J. Kim (2019). "LBD16 and LBD18 acting downstream of ARF7 and ARF19 are involved in adventitious root formation in Arabidopsis." BMC Plant Biol **19**(1): 46.
Lee, S., S. Sundaram, L. Armitage, J. P. Evans, T. Hawkes, S. Kepinski, N. Ferro and R. M. Napier (2014). "Defining binding efficiency and specificity of auxins for SCFTIR1/AFB-Aux/IAA co-receptor complex formation." ACS chemical biology **9**(3): 673-682.
Li, E., S. Wang, Y. Liu, J. G. Chen and C. J. Douglas (2011). "OVATE FAMILY PROTEIN4 (OFP4) interaction with KNAT7 regulates secondary cell wall formation in Arabidopsis thaliana." The Plant Journal **67**(2): 328-341.
Li, L., I. Verstraeten, M. Roosjen, K. Takahashi, L. Rodriguez, J. Merrin, J. Chen, L. Shabala, W. Smet and H. Ren (2021). "Cell surface and intracellular auxin signalling for H+ fluxes in root growth." Nature **599**(7884): 273-277.
Liu, Y. and C. J. Douglas (2015). "A role for OVATE FAMILY PROTEIN1 (OFP1) and OFP4 in a BLH6-KNAT7 multi-protein complex regulating secondary cell wall formation in Arabidopsis thaliana." Plant signaling & behavior **10**(7): e1033126.
Luschnig, C., R. A. Gaxiola, P. Grisafi and G. R. Fink (1998). "EIR1, a root-specific protein involved in auxin transport, is required for gravitropism inArabidopsis thaliana." Genes & development **12**(14): 2175-2187.
Lynch, J. (1995). "Root architecture and plant productivity." Plant physiology **109**(1): 7.
Ma, Q., P. Grones and S. Robert (2017). "Auxin signaling: a big question to be addressed by small molecules." Journal of Experimental Botany **69**(2): 313-328.
Ma, Y., C. Yang, Y. He, Z. Tian and J. Li (2017). "Rice OVATE family protein 6 regulates plant development and confers resistance to drought and cold stresses." Journal of Experimental Botany **68**(17): 4885-4898.
Malamy, J. E. and P. N. Benfey (1997). "Organization and cell differentiation in lateral roots of Arabidopsis thaliana." Development **124**(1): 33-44.
Mhimdi, M. and J. M. Pérez-Pérez (2020). "Understanding of adventitious root formation: what can we learn from comparative genetics?" Frontiers in plant science **11**: 582020.
Moreno-Risueno, M. A., J. M. Van Norman, A. Moreno, J. Zhang, S. E. Ahnert and P. N. Benfey (2010). "Oscillating gene expression determines competence for periodic Arabidopsis root branching." Science **329**(5997): 1306-1311.
Moreno-Risueno, M. A., J. M. Van Norman, A. Moreno, J. Zhang, S. E. Ahnert and P. N. Benfey (2010). "Oscillating gene expression determines competence for periodic Arabidopsis root branching." Science **329**(5997): 1306-1311.
Nagpal, P., L. M. Walker, J. C. Young, A. Sonawala, C. Timpte, M. Estelle and J. W. Reed (2000). "AXR2 encodes a member of the Aux/IAA protein family." Plant Physiol **123**(2): 563-574.
Nissen, S. J. and E. G. Sutter (1990). "Stability of IAA and IBA in nutrient medium to several tissue culture procedures." HortScience **25**(7): 800-802.
Okushima, Y., H. Fukaki, M. Onoda, A. Theologis and M. Tasaka (2007). "ARF7 and ARF19 regulate lateral root formation via direct activation of LBD/ASL genes in Arabidopsis." The Plant Cell **19**(1): 118-130.
Okushima, Y., P. J. Overvoorde, K. Arima, J. M. Alonso, A. Chan, C. Chang, J. R. Ecker, B. Hughes, A. Lui and D. Nguyen (2005). "Functional genomic analysis of the AUXIN RESPONSE FACTOR gene family members in Arabidopsis thaliana: unique and overlapping functions of ARF7 and ARF19." The Plant Cell **17**(2): 444-463.
Omary, M., N. Gil-Yarom, C. Yahav, E. Steiner, A. Hendelman and I. Efroni (2022). "A conserved superlocus regulates above-and belowground root initiation." Science **375**(6584): eabf4368.

Overvoorde, P., H. Fukaki and T. Beeckman (2010). "Auxin control of root development." Cold Spring Harbor perspectives in biology **2**(6): a001537.
Pacurar, D. I., M. L. Pacurar, J. D. Bussell, J. Schwambach, T. I. Pop, M. Kowalczyk, L. Gutierrez, E. Cavel, S. Chaabouni, K. Ljung, A. G. Fett-Neto, D. Pamfil and C. Bellini (2014). "Identification of new adventitious rooting mutants amongst suppressors of the Arabidopsis thaliana superroot2 mutation." J Exp Bot **65**(6): 1605-1618.
Paczal, A., A. C. Bényei and A. Kotschy (2006). "Modular synthesis of heterocyclic carbene precursors." The Journal of Organic Chemistry **71**(16): 5969-5979.
Pagnussat, G. C., H.-J. Yu and V. Sundaresan (2007). "Cell-fate switch of synergid to egg cell in Arabidopsis eostre mutant embryo sacs arises from misexpression of the BEL1-like homeodomain gene BLH1." The Plant Cell **19**(11): 3578-3592.
Park, S.-I., J.-J. Kim, H.-S. Kim, Y.-S. Kim and H.-S. Yoon (2021). "Enhanced glutathione content improves lateral root development and grain yield in rice plants." Plant Molecular Biology **105**: 365-383.
Parry, G., L. Calderon-Villalobos, M. Prigge, B. Peret, S. Dharmasiri, H. Itoh, E. Lechner, W. Gray, M. Bennett and M. Estelle (2009). "Complex regulation of the TIR1/AFB family of auxin receptors." Proceedings of the National Academy of Sciences **106**(52): 22540-22545.
Pei, S., Y. Liu, W. Li, B. Krichilsky, S. Dai, Y. Wang, X. Wang, D. M. Johnson, B. M. Crawford and G. B. Swift (2022). "OSCA1 is an osmotic specific sensor: a method to distinguish Ca2+ ‐ mediated osmotic and ionic perception." New Phytologist **235**(4): 1665-1678.
Quareshy, M., V. Uzunova, J. M. Prusinska and R. M. Napier (2017). Assaying auxin receptor activity using SPR assays with F-Box proteins and Aux/IAA degrons. Plant Hormones, Springer**:** 159-191.
Reed, J. W., R. P. Elumalai and J. Chory (1998). "Suppressors of an Arabidopsis thaliana phyB mutation identify genes that control light signaling and hypocotyl elongation." Genetics **148**(3): 1295-1310.
Rinaldi, M. A., J. Liu, T. A. Enders, B. Bartel and L. C. Strader (2012). "A gain-of-function mutation in IAA16 confers reduced responses to auxin and abscisic acid and impedes plant growth and fertility." Plant molecular biology **79**(4): 359-373.
Rogg, L. E., J. Lasswell and B. Bartel (2001). "A gain-of-function mutation in IAA28 suppresses lateral root development." Plant Cell **13**(3): 465-480.
Rogg, L. E., J. Lasswell and B. Bartel (2001). "A gain-of-function mutation in IAA28 suppresses lateral root development." The Plant Cell **13**(3): 465-480.
Ruegger, M., E. Dewey, W. M. Gray, L. Hobbie, J. Turner and M. Estelle (1998). "The TIR1 protein of Arabidopsis functions in auxin response and is related to human SKP2 and yeast grr1p." Genes & development **12**(2): 198-207.
Santner, A. A. and J. C. Watson (2006). "The WAG1 and WAG2 protein kinases negatively regulate root waving in Arabidopsis." The Plant Journal **45**(5): 752-764.
Savaldi-Goldstein, S., T. J. Baiga, F. Pojer, T. Dabi, C. Butterfield, G. Parry, A. Santner, N. Dharmasiri, Y. Tao and M. Estelle (2008). "New auxin analogs with growth-promoting effects in intact plants reveal a chemical strategy to improve hormone delivery." Proceedings of the National Academy of Sciences **105**(39): 15190-15195.
Scholz, S., J. Pleßmann, B. Enugutti, R. Hüttl, K. Wassmer and K. Schneitz (2019). "The AGC protein kinase UNICORN controls planar growth by attenuating PDK1 in Arabidopsis thaliana." PLoS Genetics **15**(2): e1007927.
Smith, D. L. and N. V. Fedoroff (1995). "LRP1, a gene expressed in lateral and adventitious root primordia of arabidopsis." The Plant Cell **7**(6): 735-745.

Snouffer, A., C. Kraus and E. van der Knaap (2020). "The shape of things to come: ovate family proteins regulate plant organ shape." Current opinion in plant biology **53**: 98-105.
Sorin, C., J. D. Bussell, I. Camus, K. Ljung, M. Kowalczyk, G. Geiss, H. McKhann, C. Garcion, H. Vaucheret and G. Sandberg (2005). "Auxin and light control of adventitious rooting in Arabidopsis require ARGONAUTE1." The Plant Cell **17**(5): 1343-1359.
Spartz, A. K., S. H. Lee, J. P. Wenger, N. Gonzalez, H. Itoh, D. Inzé, W. A. Peer, A. S. Murphy, P. J. Overvoorde and W. M. Gray (2012). "The SAUR19 subfamily of SMALL AUXIN UP RNA genes promote cell expansion." The Plant Journal **70**(6): 978-990.
Stöckle, D., B. J. Reyes-Hernández, A. V. Barro, M. Nenadić, Z. Winter, S. Marc-Martin, L. Bald, R. Ursache, S. Fujita and A. Maizel (2022). "Microtubule-based perception of mechanical conflicts controls plant organ morphogenesis." Science Advances **8**(6): eabm4974.
Sun, N., J. Wang, Z. Gao, J. Dong, H. He, W. Terzaghi, N. Wei, X. W. Deng and H. Chen (2016). "Arabidopsis SAURs are critical for differential light regulation of the development of various organs." Proceedings of the National Academy of Sciences **113**(21): 6071-6076.
Takahashi, F., K. Sato-Nara, K. Kobayashi, M. Suzuki and H. Suzuki (2003). "Sugar-induced adventitious roots in Arabidopsis seedlings." Journal of plant research **116**: 83-91.
Tatematsu, K., S. Kumagai, H. Muto, A. Sato, M. K. Watahiki, R. M. Harper, E. Liscum and K. T. Yamamoto (2004). "MASSUGU2 encodes Aux/IAA19, an auxin-regulated protein that functions together with the transcriptional activator NPH4/ARF7 to regulate differential growth responses of hypocotyl and formation of lateral roots in Arabidopsis thaliana." The Plant Cell **16**(2): 379-393.
Todd, O. E., M. R. Figueiredo, S. Morran, N. Soni, C. Preston, M. F. Kubeš, R. Napier and T. A. Gaines (2020). "Synthetic auxin herbicides: finding the lock and key to weed resistance." Plant Science **300**: 110631.
Ulmasov, T., J. Murfett, G. Hagen and T. J. Guilfoyle (1997). "Aux/IAA proteins repress expression of reporter genes containing natural and highly active synthetic auxin response elements." The Plant Cell **9**(11): 1963-1971.
Vain, T., S. Raggi, N. Ferro, D. K. Barange, M. Kieffer, Q. Ma, S. M. Doyle, M. Thelander, B. Pařízková and O. Novák (2019). "Selective auxin agonists induce specific AUX/IAA protein degradation to modulate plant development." Proceedings of the National Academy of Sciences **116**(13): 6463-6472.
van den Berg, T., K. Yalamanchili, H. De Gernier, J. S. Teixeira, T. Beeckman, B. Scheres, V. Willemsen and K. Ten Tusscher (2021). "A reflux-and-growth mechanism explains oscillatory patterning of lateral root branching sites." Developmental Cell **56**(15): 2176-2191. e2110.
van der Knaap, E., M. Chakrabarti, Y. H. Chu, J. P. Clevenger, E. Illa-Berenguer, Z. Huang, N. Keyhaninejad, Q. Mu, L. Sun and Y. Wang (2014). "What lies beyond the eye: the molecular mechanisms regulating tomato fruit weight and shape." Frontiers in Plant Science **5**: 227.
Vanneste, S. and J. Friml (2009). "Auxin: a trigger for change in plant development." Cell **136**(6): 1005-1016.
Vermeer, J. E., D. von Wangenheim, M. Barberon, Y. Lee, E. H. Stelzer, A. Maizel and N. Geldner (2014). "A spatial accommodation by neighboring cells is required for organ initiation in Arabidopsis." Science **343**(6167): 178-183.
Wang, J.-W., L.-J. Wang, Y.-B. Mao, W.-J. Cai, H.-W. Xue and X.-Y. Chen (2005). "Control of root cap formation by microRNA-targeted auxin response factors in Arabidopsis." The Plant Cell **17**(8): 2204-2216.
Wang, S., Y. Chang, J. Guo and J. G. Chen (2007). "Arabidopsis Ovate Family Protein 1 is a transcriptional repressor that suppresses cell elongation." The Plant Journal **50**(5): 858-872.

Wang, S., Y. Chang, J. Guo, Q. Zeng, B. E. Ellis and J.-G. Chen (2011). "Arabidopsis ovate family proteins, a novel transcriptional repressor family, control multiple aspects of plant growth and development." PLoS One **6**(8): e23896.
Wang, S., M. Yamaguchi, E. Grienenberger, P. T. Martone, A. L. Samuels and S. D. Mansfield (2020). "The Class II KNOX genes KNAT3 and KNAT7 work cooperatively to influence deposition of secondary cell walls that provide mechanical support to Arabidopsis stems." The Plant Journal **101**(2): 293-309.
Wang, X., R. Yu, J. Wang, Z. Lin, X. Han, Z. Deng, L. Fan, H. He, X. W. Deng and H. Chen (2020). "The asymmetric expression of SAUR genes mediated by ARF7/19 promotes the gravitropism and phototropism of plant hypocotyls." Cell reports **31**(3): 107529.
Wang, Y., J. P. Clevenger, E. Illa-Berenguer, T. Meulia, E. van der Knaap and L. Sun (2019). "A comparison of sun, ovate, fs8. 1 and auxin application on tomato fruit shape and gene expression." Plant and Cell Physiology **60**(5): 1067-1081.
Welander, M., T. Geier, A. Smolka, A. Ahlman, J. Fan and L. H. Zhu (2014). "Origin, timing, and gene expression profile of adventitious rooting in Arabidopsis hypocotyls and stems." American Journal of Botany **101**(2): 255-266.
Willige, B. C., S. Ahlers, M. Zourelidou, I. C. Barbosa, E. Demarsy, M. Trevisan, P. A. Davis, M. R. G. Roelfsema, R. Hangarter and C. Fankhauser (2013). "D6PK AGCVIII kinases are required for auxin transport and phototropic hypocotyl bending in Arabidopsis." The Plant Cell **25**(5): 1674-1688.
Wilson, A. K., F. B. Pickett, J. C. Turner and M. Estelle (1990). "A dominant mutation inArabidopsis confers resistance to auxin, ethylene and abscisic acid." Molecular and General Genetics MGG **222**(2): 377-383.
Xiao, Z., N. Ji, X. Zhang, Y. Zhang, Y. Wang, T. Wu, X. Xu and Z. Han (2014). "The lose of juvenility elicits adventitious rooting recalcitrance in apple rootstocks." Plant Cell, Tissue and Organ Culture (PCTOC) **119**(1): 51-63.
Xu, T., N. Dai, J. Chen, S. Nagawa, M. Cao, H. Li, Z. Zhou, X. Chen, R. De Rycke and H. Rakusová (2014). "Cell surface ABP1-TMK auxin-sensing complex activates ROP GTPase signaling." Science **343**(6174): 1025-1028.
Xuan, W., D. Audenaert, B. Parizot, B. K. Möller, M. F. Njo, B. De Rybel, G. De Rop, G. Van Isterdael, A. P. Mähönen and S. Vanneste (2015). "Root cap-derived auxin pre-patterns the longitudinal axis of the Arabidopsis root." Current Biology **25**(10): 1381-1388.
Xuan, W., L. R. Band, R. P. Kumpf, D. Van Damme, B. Parizot, G. De Rop, D. Opdenacker, B. K. Möller, N. Skorzinski and M. F. Njo (2016). "Cyclic programmed cell death stimulates hormone signaling and root development in Arabidopsis." Science **351**(6271): 384-387.
Yang, C., W. Shen, Y. He, Z. Tian and J. Li (2016). "OVATE family protein 8 positively mediates brassinosteroid signaling through interacting with the GSK3-like kinase in rice." PLoS Genetics **12**(6): e1006118.
Yang, X., S. Lee, J. h. So, S. Dharmasiri, N. Dharmasiri, L. Ge, C. Jensen, R. Hangarter, L. Hobbie and M. Estelle (2004). "The IAA1 protein is encoded by AXR5 and is a substrate of SCFTIR1." The Plant Journal **40**(5): 772-782.
Zeng, Y., S. Schotte, H. K. Trinh, I. Verstraeten, J. Li, E. Van de Velde, S. Vanneste and D. Geelen (2022). "Genetic Dissection of Light-Regulated Adventitious Root Induction in Arabidopsis thaliana Hypocotyls." International Journal of Molecular Sciences **23**(10): 5301.
Zhang, H., A. Jennings, P. W. Barlow and B. G. Forde (1999). "Dual pathways for regulation of root branching by nitrate." Proceedings of the National Academy of Sciences **96**(11): 6529-6534.

Zhao, Y., S. Araki, J. Wu, T. Teramoto, Y.-F. Chang, M. Nakano, A. S. Abdelfattah, M. Fujiwara, T. Ishihara and T. Nagai (2011). "An expanded palette of genetically encoded Ca2+ indicators." Science **333**(6051): 1888-1891.
Zimmerman, P. W. (1935). "Several chemical growth substances which cause initiation of roots and other responses in plants." Contrib. Boyce Thompson Inst. **7**: 209-229.
Zourelidou, M., B. Absmanner, B. Weller, I. C. Barbosa, B. C. Willige, A. Fastner, V. Streit, S. A. Port, J. Colcombet and S. de la Fuente van Bentem (2014). "Auxin efflux by PIN-FORMED proteins is activated by two different protein kinases, D6 PROTEIN KINASE and PINOID." Elife **3**: e02860.

Figures

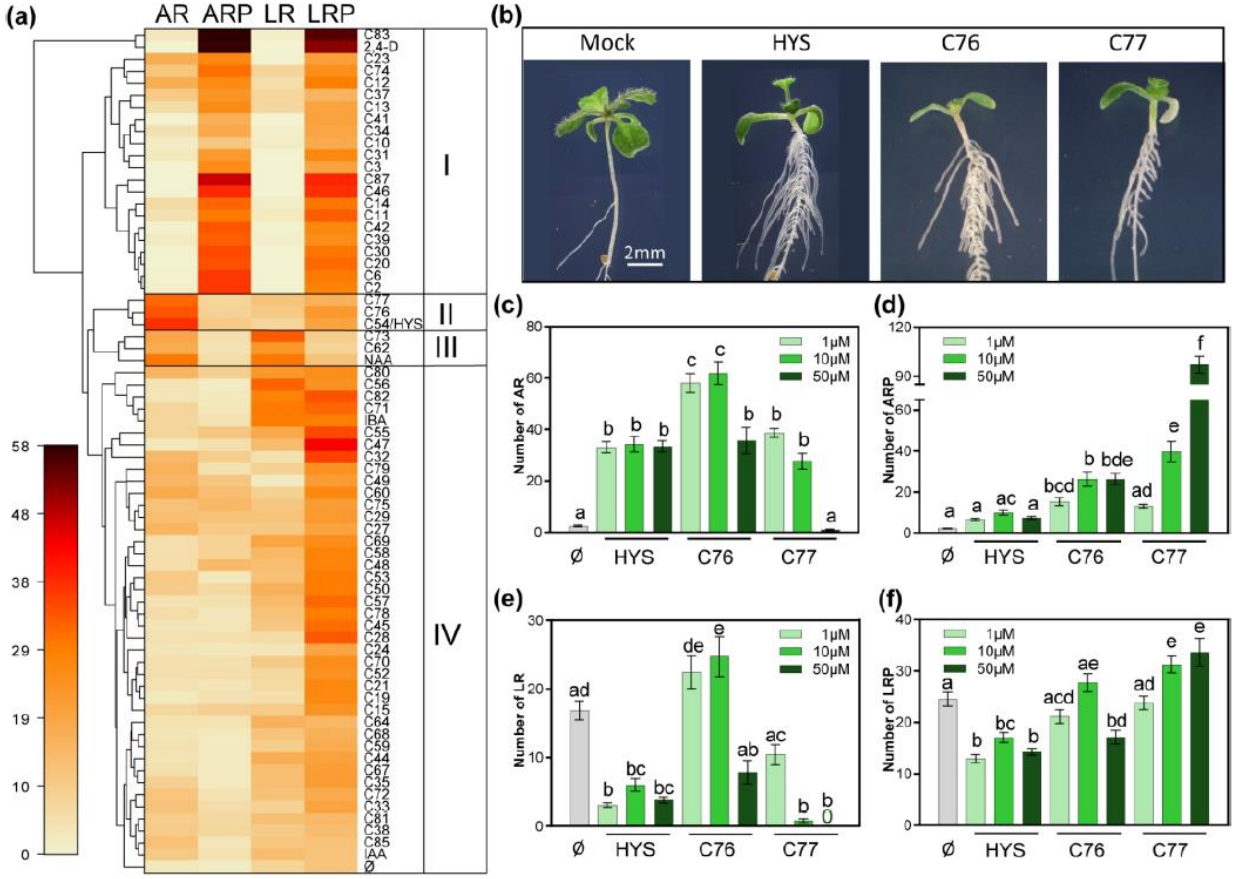

Figure 1 Identification and validation of HYSPARIN

(a) Hierarchical clustering of biological activities of the tested compounds, as positive controls, IAA, IBA, NAA and 2,4-D were included (10µM). Mock treatment (Ø) is DMSO (0.1%). Etiolated seedlings were subjected to indicated treatments for 10 days before quantification AR = Adventitious Roots, ARP = Adventitious Root Primordia, LR = Lateral Root, LRP = Lateral Root Primordia. Data represent averages of ≥20 seedlings. **(b)** Representative images of the hypocotyl AR phenotype of 10-day old, etiolated seedlings treated with or without 10 µM compounds, mock, HYS, C76 and C76. Scale bar is 2mm. **(c-f)** Quantification of number of AR **(c)**, ARP **(d)**, LR **(e)** and LRP **(f)** of the group II compounds at 1 µM, 10 µM and 50 µM compared to mock (Ø). Etiolated seedlings (3 days after germination) were subjected to indicated treatments for 10 days before quantification. Data are presented as mean values ± SE (n≥20), ANOVA and LSD *post-hoc* analysis, Different lettering indicates statistical differences at $p < 0.05$.

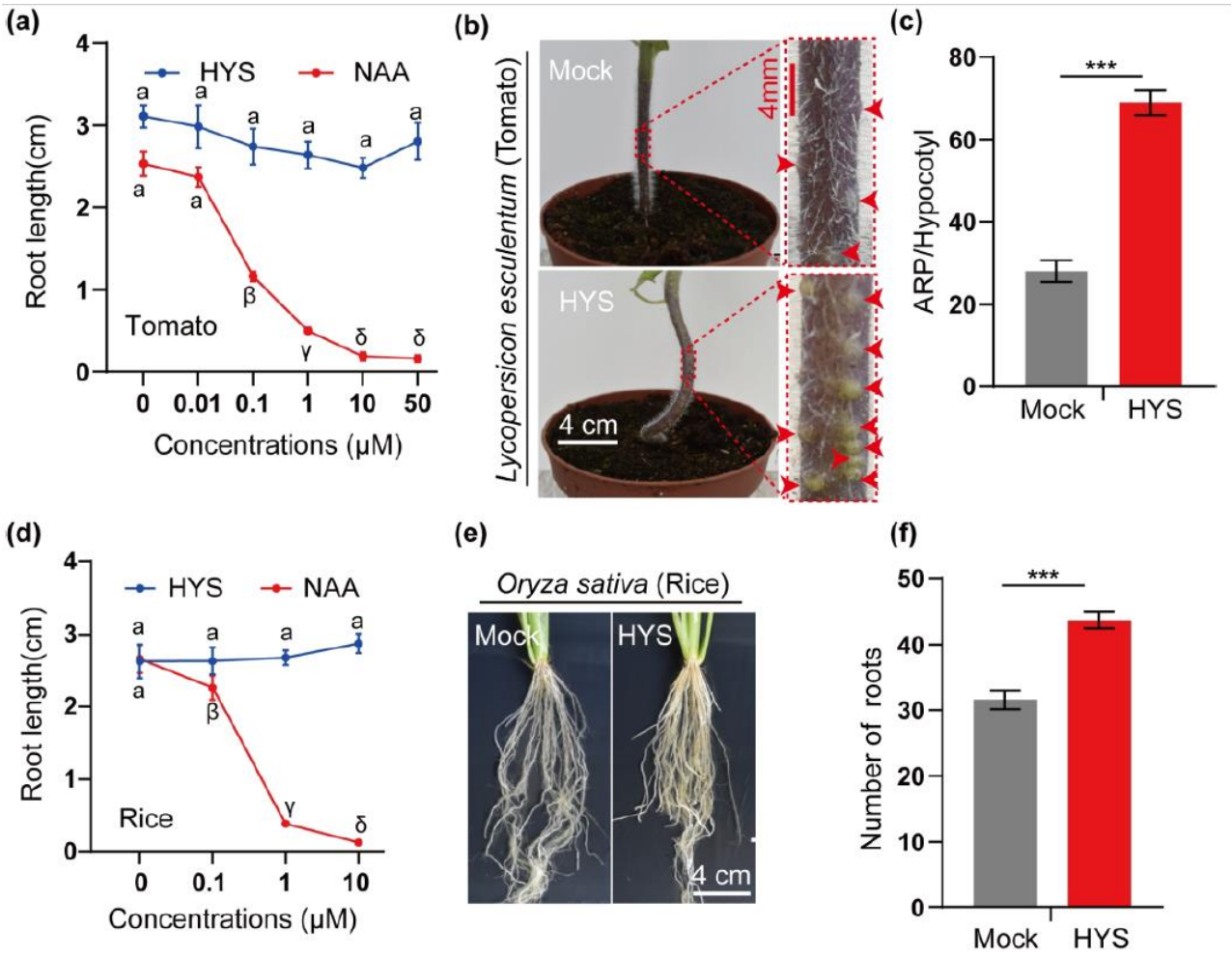

Figure 2 Application of HYS induces root formation in tomato and rice.

(a) Dose-response curves for HYS and NAA on tomato primary root growth. Three-day-old, etiolated tomato (Ailsa Craig) seedlings were transferred to media with NAA or HYS and root length increment was measured 5 days after transfer. **(b-c)** Foliar spray application of HYS to the four-day-old cotyledons induced AR formation in tomato (Ailsa Craig) hypocotyls. **(b)** Phenotype of the 4-week-old tomato hypocotyl treated with HYS or mock showing emerged AR; inset in panel shows close-up of hypocotyl ARP indicated by red arrowhead. **(c)** Quantification of ARP as shown in **(b);** Data are presented as averages ±SE (mock, *n*=17; HYS, *n*=19). **(d)** Dose-response for HYS and NAA on rice primary root growth. Three-day-old rice seedlings were transferred to media with NAA or HYS and root length increment was measured 3 days after transfer. **(e-f)** Foliar spray application of HYS to four-day-old seedlings induces nodal root formation of rice. **(e)** Root phenotype of the 4-week-old-rice. **(f)** Quantification of number of roots as shown in **(e);** Data are presented as averages ±SE (mock, *n*=17; HYS, *n*=17). (***: $p \leq 0.001$, unpaired Student's t-test). **(a, d)** HYS or NAA

concentrations as indicated; Data represent averages of $n \geqslant 10$ seedlings. Letters indicate statistical differences at p<0.05 (ANOVA and LSD *post-hoc* analysis).

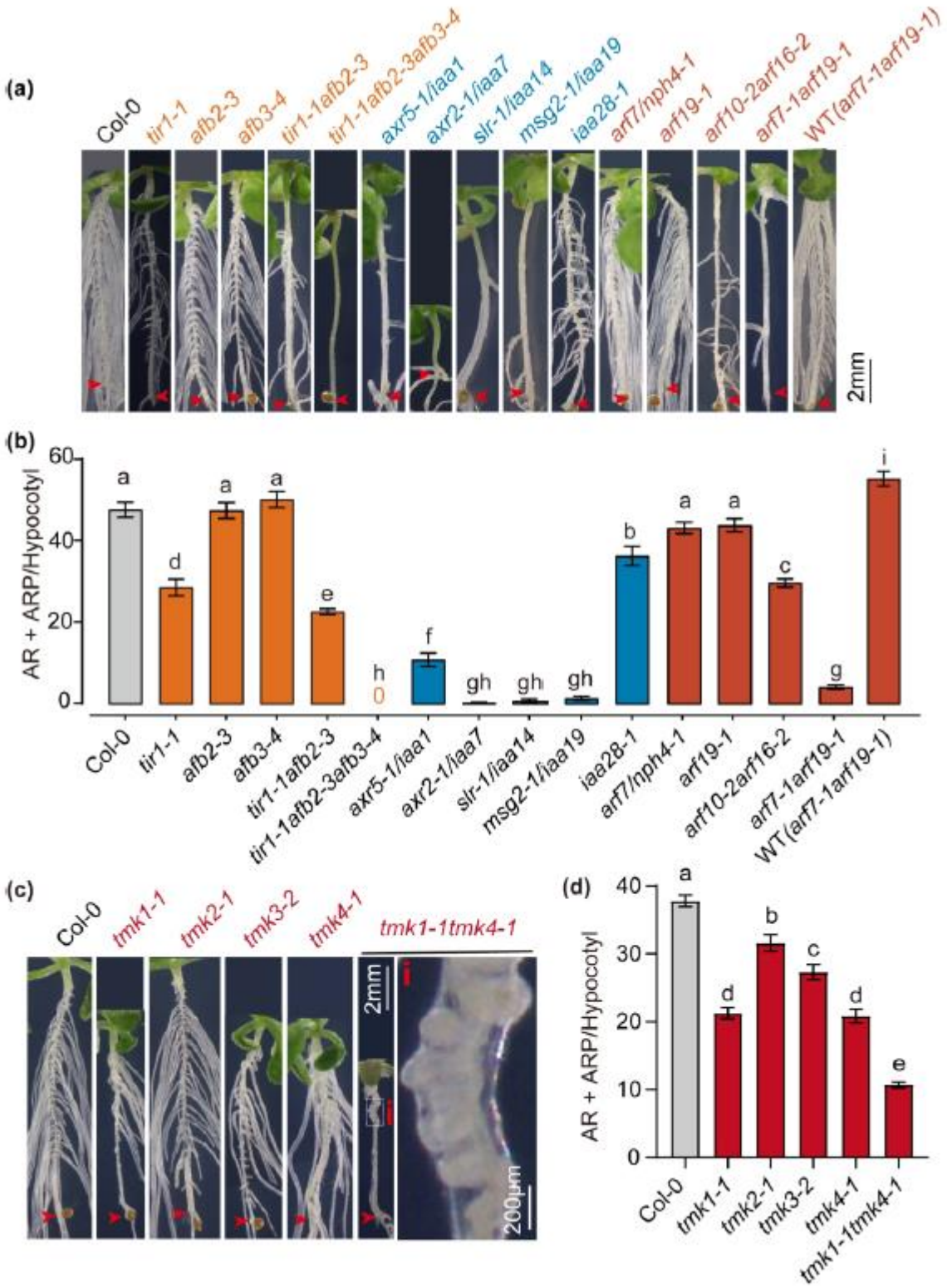

Figure 3 HYS induces AR formation through a nuclear and a plasma membrane auxin signalling pathway.

(a) Hypocotyl AR phenotype of etiolated seedlings treated with 10 µM HYS for 10 days after etiolation. Due to the presence of *DR5::LUC* in the *arf7-1arf19-1* background, DR5::LUC was included as a control for *arf7-1arf19-1*. **(b)** Quantification of AR and ARP of the seedlings as in **(a)**; Means ± SEM are shown, (n>20). **(c)** Hypocotyl AR phenotype of etiolated seedlings of *tmk1-1, tmk2-1, tmk3-2, tmk4-1*, double *tmk1-1tmk4-1* mutants, relative to Col-0 (WT). Close up of the boxed area of *tmk1-1tmk4-1* (i). **(d)** Quantification of the AR and ARP of the seedlings as in **(c)**; Means ± SEM are shown, (n>20). Red arrowhead points to the hypocotyl root junction. Scale bar is 2mm. Letters indicate statistical differences at $p<0.05$ (ANOVA and LSD *post-hoc* analysis).

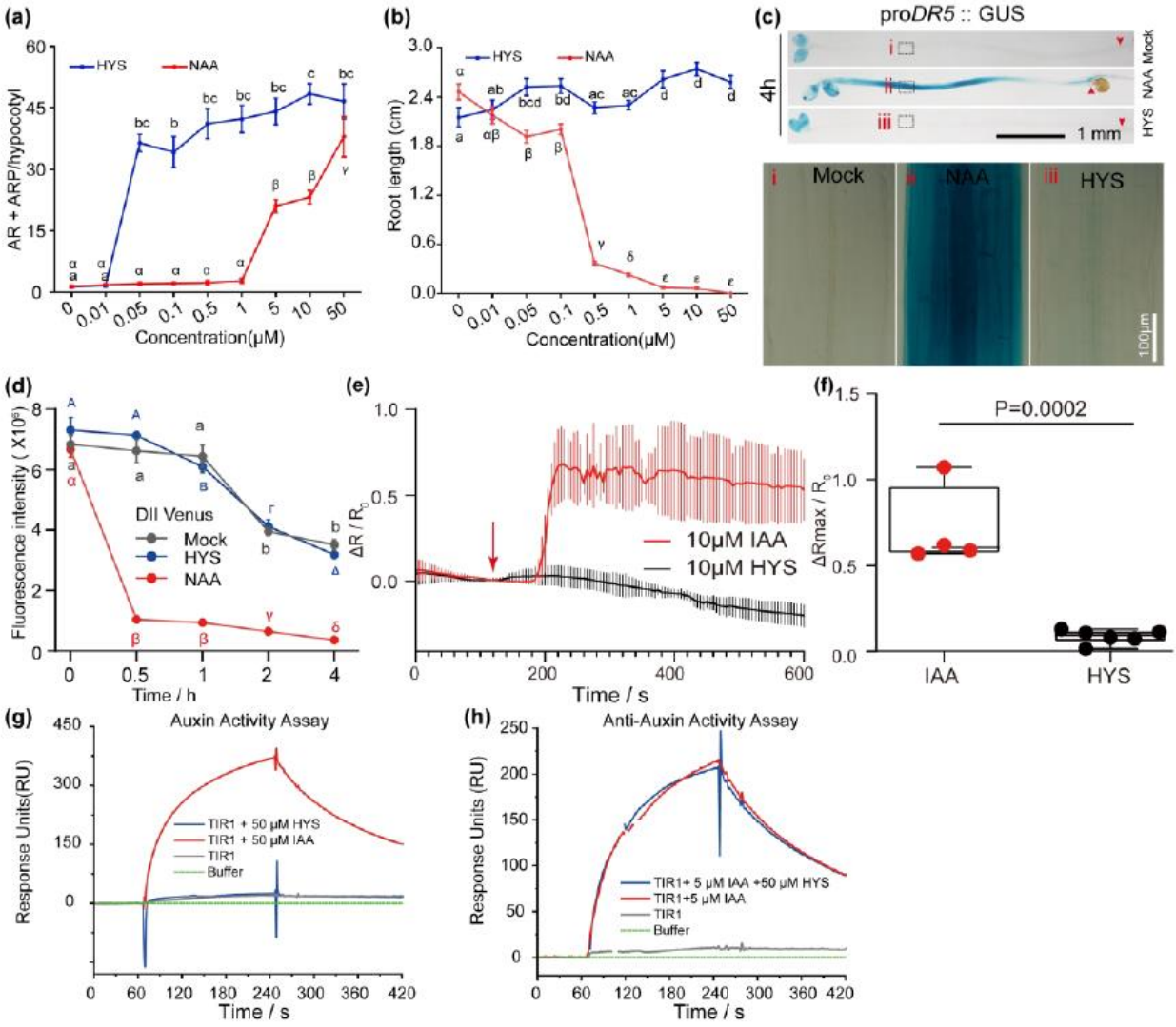

Figure 4. HYS is not a classical synthetic auxin.

(a) Number of ARP and **(b)** primary root length in response do different doses of HYS and NAA after 3 days incubation. Values are the mean ± SE; Data represent averages of ≥10 seedlings. Different letter indicates statistical differences at P<0.05, ANOVA and LSD post-hoc analysis. **(c)** The auxin response in etiolated hypocotyls expressing the *proDR5::GUS* reporter treated for 4 hours with HYS (10 μM) or NAA (10 μM). Scale bar is 100μm. Red arrowhead points to the hypocotyl root junction. i, ii and iii are magnification images corresponding to the boxed areas. Scale bar is 1mm. **(d)** Quantification of the time-course response of DII-VENUS fluorescence signal in root tips treated with HYS (10 μM) or NAA (10 μM), Mock is DMSO (0.1%). Values are the mean ± SE, *n*=4. Different letter indicates statistical differences at P<0.05, ANOVA and LSD post-hoc analysis. **(e)** Average and normalized YC-Nano65 fluorescence intensities over time upon treatment with 10μM HYS or 10μM IAA in the five-day old root vascular tissue. Values are the means ± SD; HYS, *n*=6; IAA, *n*=4, unpaired Student's t-test. HYS or IAA treatments were applied time points as indicated. **(f)** Boxplot

representation of the maximal amplitude of the treatments described in **(e)**. **(g)** Analysis of HYS auxin activity by surface plasmon resonance. **(h)** Analysis of HYS anti-auxin activity by surface plasmon resonance. All the surface plasmon resonance assays were run under standard conditions of 25 °C, flow rate 20 µL/min in HEPES-buffered saline with Tween 20 (20 mM Hepes, 150 mM NaCl, 3 mM EDTA + 0.01% Tween 20). Compounds were dissolved in DMSO as 10mM stocks and added to the assay to give 50 µM final concentration and a sub-stock of IAA at 1 mM in DMSO was used for the antiauxin experiment. DMSO was added to the buffer at the same final concentration (0.5%) with no protein for the experimental baseline. For testing for auxin activity, HYS and IAA were tested at 50 µM. For testing anti-auxin activity, IAA was used at 5 µM and HYS added at 50 µM.

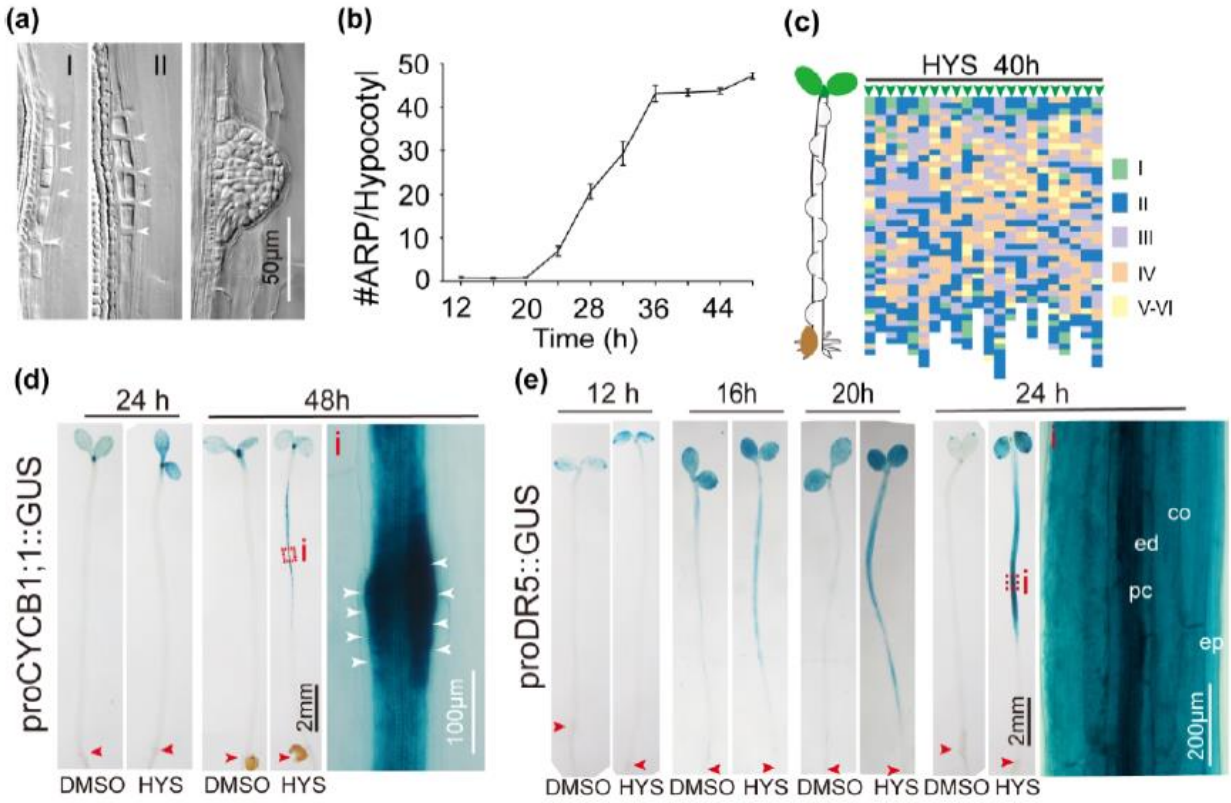

Figure 5 Characterisation of HYS-induced AR formation.

(a) Different stages of AR development after HYS treatment. Stage I, anticlinal cell divisions in the pericycle layer in perpendicular orientation to hypocotyl axis; Stage II, a periclinal cell division occurs giving rise to two layers of the primordium. White arrowheads point to cell walls from anticlinal or oblique cell divisions. Scale bar is 50 µm. **(b)** Dynamics of HYS-induced ARP formation in WT (Col-0) over time. Values are the mean ± SE, n⩾10. **(c)** Schematic representation of the individual distribution of HYS-induced ARPs along the etiolated hypocotyls after transfer in the light for 40 hours (n=22). Green triangles indicate individual seedlings. The colour code corresponds to different ARP stages as indicated. **(d)** Activation of the G2/M reporter *proCYCB1;1::GUS* in etiolated hypocotyls, after 24h and 48 h DMSO (0.1 %) and HYS (10 µM) treatment. A close- up (i) shows the induction of the reporter in dividing pericycle cells. White arrowheads indicate dividing cells. The scale bar is 2 mm in the original images and 100 µm in the close-up. **(e)** Time-course of *proDR5: GUS* in etiolated hypocotyls treated with DMSO (0.1%) or HYS (10 µM) for 12 h, 16 h, 20 h and 24 h. Insets i show a close-up of tissue with GUS expression. Scale bar is 1mm. pc, pericycle; ed, endodermis; co, cortex and ep, epidermis. Scale bar is 200µm. Red arrowhead points to the hypocotyl root junction. Scale bar is 2mm.

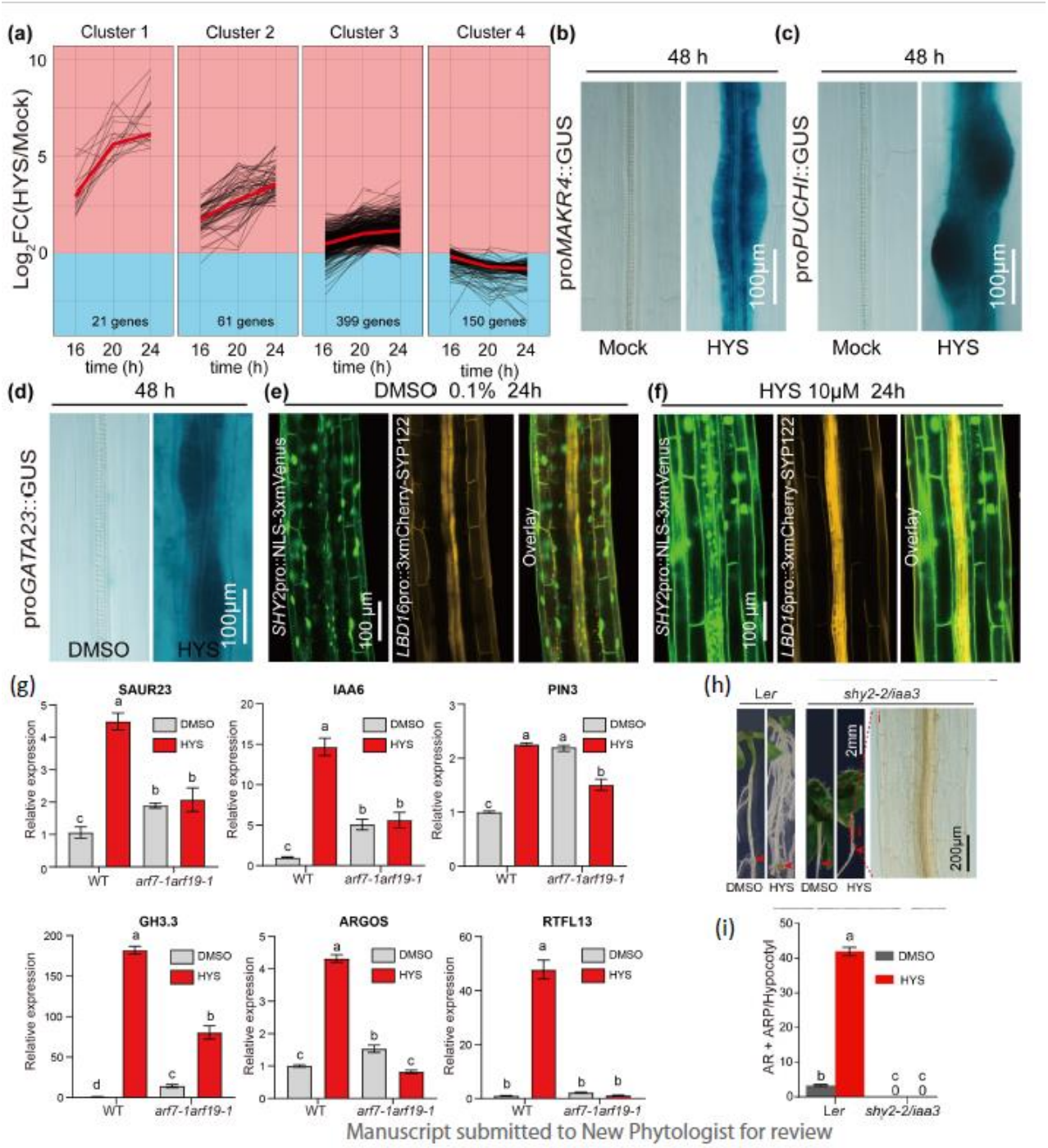

Figure 6 Transcriptome analysis of HYS-induced AR formation.

(a) Hierarchical clustering of expression profiles of HYS-regulated genes. Each black line displays the log2 fold change of one differentially expressed gene (FDR < 0.05) after HYS treatment for 16 h, 20 h and 24 h compared to the corresponding mock sample. Red lines represent the median of each cluster. **(b-d)** HYS-responsive activity of **(b)** *proMAKR4::GUS*, **(c)** *proPUCHI::GUS* and (d) *proGATA23::GUS* after 48h 10 µM HYS treatment in etiolated seedlings. Scale bar is 100µm. **(e-f)** Confocal image of a hypocotyl expressing *proSHY2*::NLS-3xmVenus (green), *LBD16*pro::3xmCherry-

SYP122 (yellow), autofluorescence (red) and overlay after 24h 10µM HYS treatment **(f)** in etiolated seedlings compared to the mock treatment **(e)**. Scale bar is 100µm. Seedlings were etiolated for three days before transfer to HYS. **(g)** Q-PCR with hypocotyl RNA from three-day-old, etiolated Arabidopsis Col-0 and arf7-1arf19-1 seedlings after 10 µM HYS or 0.1% DMSO treatment for 24 h. Data are the mean ± SD of three biological replicates. Letters indicate statistical differences at $p<0.05$ (ANOVA and LSD *post-hoc* analysis). UBQ1 and ACT2 were used as internal control. **(h)** AR phenotype of etiolated *shy2-2/iaa3* seedlings treated with 10 µM HYS for 10 days. The inset i shows a close-up of a cleared hypocotyl. Wild type (L*er*) is included for comparison and red arrowheads point to the hypocotyl-root junction. The scale bar is 2 mm and 200 µm in the close-up. **(i)** Quantification of the AR and ARP of the seedlings as shown in **(h)**. Values are the mean ± SE; ($n\geq20$).

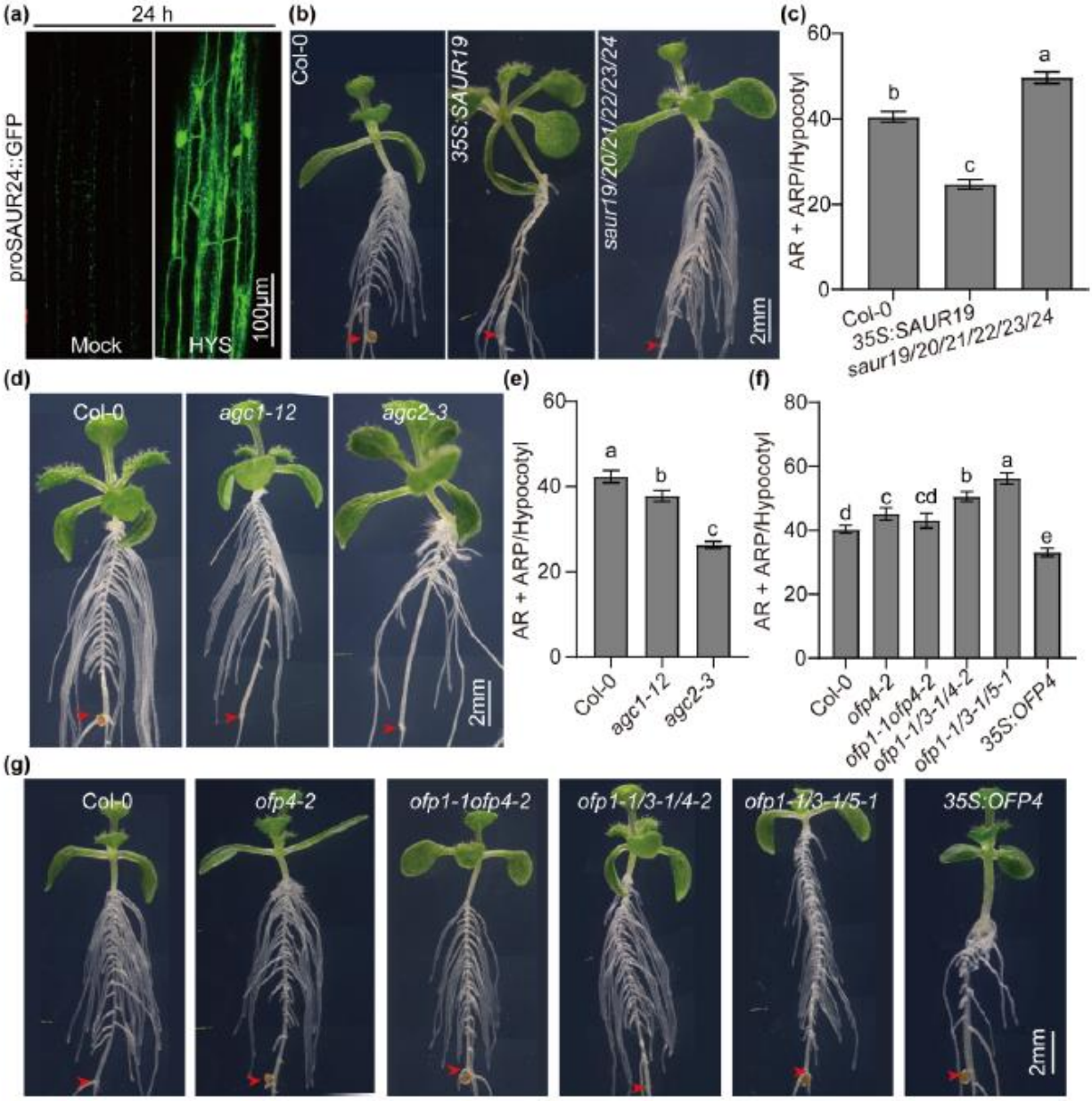

Figure 7. HYS-induced adventitious rooting in SAUR19, OFP and agc2-3 mutants.

(a) Fluorescence of GFP-tagged SAUR24 expressed under the control of native promoter predominantly in the hypocotyls of Arabidopsis seedlings. Fluorescent signals were assessed by confocal microscopy in the hypocotyls of 3-day-old dark-grown seedlings after 24h treated with 10 µM HYS. Bars, 100 µm. **(b)** Representative hypocotyl AR phenotype of etiolated seedlings of wild type (Col-0), *35S::SAUR19*, and *saur19/20/21/22/23/24* sextuple mutant. **(c)** Quantification of the AR and ARP of the seedlings as shown in **(b)**; Means ± SEM are shown, (Col-0, *n*=29, 35S::SAUR19, *n*=20; *saur19/20/21/22/23/24*, *n*=33). **(d)** Representative hypocotyl AR phenotype of etiolated seedlings of *agc1-12* (FLAG_584B10) and *agc2-3* (SALK_044862C) mutants, relative to wild type (Col-0). **(e)** Quantification of the AR and ARP of the seedlings as shown in **(d)**; Means ± SEM are

shown, (Col-0, *n*=38, agc1-12, *n*=37; *agc2-3*, *n*=43). **(f)** Quantification of the AR and ARP of the seedlings as shown in **(g)**; **(g)** Representative hypocotyl AR phenotype of etiolated seedlings of *ofp4-2*, *ofp1-1ofp4-2*, triple *ofp1-1/3-1/4-2* , triple *ofp1-1/3-1/5-1* mutants and *35S::OFP4*, wild type (Col-0) is included; Means ± SEM are shown, (Col-0, *n*=30; *ofp4-2*,*n*=20; *ofp1-1ofp4-2*,*n*=19; *ofp1-1/3-1/4-2*, *n*=19; *ofp1-1/3-1/5-1, n=20; 35S::OFP4, n=20*). All treatments are 10 µM HYS for 10 days after 3 days of etiolation. Red arrowheads point to the hypocotyl root junction. Scale bar is 2mm. Letters indicate statistical differences at $p<0.05$ (ANOVA and LSD *post-hoc* analysis).